43417

National Library of Canada / Bibliothèque nationale du Canada

CANADIAN THESES ON MICROFICHE / THÈSES CANADIENNES SUR MICROFICHE

NAME OF AUTHOR/*NOM DE L'AUTEUR* ANDREW G. GRAHAM

TITLE OF THESIS/*TITRE DE LA THÈSE* THE THERMAL STABILITY OF SUPPORTED BIMETALLIC CATALYSTS

UNIVERSITY/*UNIVERSITÉ* UNIVERSITY OF ALBERTA

DEGREE FOR WHICH THESIS WAS PRESENTED/ *GRADE POUR LEQUEL CETTE THÈSE FUT PRÉSENTÉE* M. Sc.

YEAR THIS DEGREE CONFERRED/*ANNÉE D'OBTENTION DE CE GRADE* 1978

NAME OF SUPERVISOR/*NOM DU DIRECTEUR DE THÈSE* DR. S. E. WANKE

Permission is hereby granted to the NATIONAL LIBRARY OF CANADA to microfilm this thesis and to lend or sell copies of the film.

The author reserves other publication rights, and neither the thesis nor extensive extracts from it may be printed or otherwise reproduced without the author's written permission.

L'autorisation est, par la présente, accordée à la BIBLIOTHÈQUE NATIONALE DU CANADA de microfilmer cette thèse et de prêter ou de vendre des exemplaires du film.

L'auteur se réserve les autres droits de publication; ni la thèse ni de longs extraits de celle-ci ne doivent être imprimés ou autrement reproduits sans l'autorisation écrite de l'auteur.

DATED/*DATÉ* Oct 5/78 SIGNED/*SIGNÉ* Andrew Graham

PERMANENT ADDRESS/*RÉSIDENCE FIXÉ* R.R. 6 (PLEASANT POINT)
LINDSAY, ONTARIO K9V 4R6

NL-91 (3-74)

National Library of Canada

Cataloguing Branch
Canadian Theses Division

Ottawa, Canada
K1A 0N4

Bibliothèque nationale du Canada

Direction du catalogage
Division des thèses canadiennes

NOTICE

The quality of this microfiche is heavily dependent upon the quality of the original thesis submitted for microfilming. Every effort has been made to ensure the highest quality of reproduction possible.

If pages are missing, contact the university which granted the degree.

Some pages may have indistinct print especially if the original pages were typed with a poor typewriter ribbon or if the university sent us a poor photocopy.

Previously copyrighted materials (journal articles, published tests, etc.) are not filmed.

Reproduction in full or in part of this film is governed by the Canadian Copyright Act, R.S.C. 1970, c. C-30. Please read the authorization forms which accompany this thesis.

THIS DISSERTATION
HAS BEEN MICROFILMED
EXACTLY AS RECEIVED

AVIS

La qualité de cette microfiche dépend grandement de la qualité de la thèse soumise au microfilmage. Nous avons tout fait pour assurer une qualité supérieure de reproduction.

S'il manque des pages, veuillez communiquer avec l'université qui a conféré le grade.

La qualité d'impression de certaines pages peut laisser à désirer, surtout si les pages originales ont été dactylographiées à l'aide d'un ruban usé ou si l'université nous a fait parvenir une photocopie de mauvaise qualité.

Les documents qui font déjà l'objet d'un droit d'auteur (articles de revue, examens publiés, etc.) ne sont pas microfilmés.

La reproduction, même partielle, de ce microfilm est soumise à la Loi canadienne sur le droit d'auteur, SRC 1970, c. C-30. Veuillez prendre connaissance des formules d'autorisation qui accompagnent cette thèse.

LA THÈSE A ÉTÉ
MICROFILMÉE TELLE QUE
NOUS L'AVONS REÇUE

NL-339 (3/77)

THE UNIVERSITY OF ALBERTA

THE THERMAL STABILITY OF SUPPORTED BIMETALLIC CATALYSTS

by

ANDREW G. GRAHAM

(C)

A THESIS

SUBMITTED TO THE FACULTY OF GRADUATE STUDIES AND RESEARCH

IN PARTIAL FULFILMENT OF THE REQUIREMENTS FOR THE DEGREE

OF MASTER OF SCIENCE

IN

CHEMICAL ENGINEERING

DEPARTMENT OF CHEMICAL ENGINEERING

EDMONTON, ALBERTA

FALL, 1978

THE UNIVERSITY OF ALBERTA

FACULTY OF GRADUATE STUDIES AND RESEARCH

The undersigned certify that they have read, and recommend to the Faculty of Graduate Studies and Research, for acceptance, a thesis entitled THE THERMAL STABILITY OF SUPPORTED BIMETALLIC CATALYSTS submitted by ANDREW G. GRAHAM in partial fulfilment of the requirements for the degree of Master of Science.

S. E. Wanke (Supervisor)

I. G. Dalla Lana

T. H. Etsell

Date September 20, 1978

to my parents

ABSTRACT

The loss of metal surface area in supported metal catalysts due to thermal sintering is one of the main causes for the deactivation of the catalysts. In this study changes in metal surface area caused by thermal treatment in hydrogen and oxygen at 300 and 800 °C for 1 and 16 h were examined for monometallic catalysts (1%Pt, 1%Ir, 1%W) and bimetallic catalysts (1%Pt/1%Ir and 1%Pt/1%W) supported on alumina (Alon).

Metal surface areas were measured by hydrogen adsorption using the dynamic flow method. Support surface areas where obtained by the BET method and changes in support crystallinity were examined by X-ray diffraction.

Sintering results for the monometallic catalysts and the physical mixtures of the monometallic catalysts were obtained so that direct comparisons with the bimetallic catalysts could be made. The results for these catalysts are in general agreement with the results obtained by previous investigators, i.e. W forms a non-hydrogen adsorbing complex with alumina; metal surface areas of Pt and Ir decrease monotonically with increased sintering temperatures for treatment in hydrogen; increases in metal surface area occur for Pt and Ir during treatment in oxygen at temperatures of 300 - 550 °C for Pt and 300 - 350 °C for Ir.

The sintering results for the bimetallic catalysts

showed that interaction existed between the two metals co-impregnated on the alumina support. The sintering behaviour of the Pt/Ir bimetallic catalyst was very similar to that of the Ir catalyst when treated in hydrogen. (Note; the physical mixture of the Pt and Ir catalysts during treatment in hydrogen did not display any sinergistic effects). After treatment in oxygen for 1 h the Pt/Ir bimetallic catalyst showed interaction between the Pt and Ir. After 16 h treatment in oxygen the results were similar to those for the physical mixture of Pt and Ir catalysts. The physical mixture of Pt and Ir indicated long range interactions between the metals which is believed to be due to vapour phase transport of metal oxide species. The Pt/W system was less extensively studied than the Pt/Ir system but the results indicate a strong interaction between the Pt and W metals.

It was concluded that in the freshly prepared bimetallic catalysts the metals are not physically separated on the support surface but are in close proximity to each other (possibly alloyed).

ACKNOWLEDGEMENTS

It is a great pleasure to acknowledge those people to whom the success of this project is so indebted.

First I would like to thank Keith Faulder of the machine shop, and Don Sutherland, Reg Hartwig, Dave Hawirko of the instrument shop. I sincerely appreciated the constant co-operation, help and good advice and the great interest they showed in my work.

Also I would like to acknowledge Dave Furnell of the DACS center who helped me solve my computing problems and showed me the 'magic' of MTS. Similarly, Jerry Moser the resident department chemist, always treated my problems with the highest of priority and certainly helped to make the project run smoothly.

Special thanks to J&KH, R&BJ, SGW, RCG, BJM and good old Normie Freitag for befriending a homesick easterner.

Foremost I would like to thank Sieghard Wanke. Dr. Wanke was an excellent supervisor. He was a constant source of encouragement and advice. He was always enthusiastic about the project and was always ready to listen and talk. Appreciated most,though, was his genuine interest in my academic and personal life.

TABLE OF CONTENTS

CHAPTER		PAGE
1.	INTRODUCTION	1
	1.1 Supported Metal Catalysts	1
	1.2 Measurement of Metal Dispersion	2
	1.3 Supported Bimetallic Catalysts	3
2.	EXPERIMENTAL	6
	2.1 Introduction	6
	2.2 Catalysts Preparation	6
	2.3 Experimental Schedule	8
	2.4 Dynamic Flow Adsorption Method	9
	2.5 X-ray Diffraction Measurement	13
	2.6 BET Surface Area Measurement	15
3.	RESULTS	16
	3.1 Introduction	16
	3.2 Adsorption Results	18
	3.3 The BET Surface Area Results	19
	3.4 X-ray Diffraction Results	19
4.	DISCUSSION	33
	4.1 Introduction	33
	4.2 Factors Affecting Initial Metal Dispersion	33
	4.2.1 Choice of Metal Salt	34
	4.2.2 Choice of Support	34
	4.2.3 Choice of Reduction Treatment	35
	4.2.4 Summary	35

TABLE OF CONTENTS continued

CHAPTER		PAGE
	4.3 Hydrogen Chemisorption Measurement	36
	4.3.1 The Dynamic Flow Method	36
	4.3.2 Factors Inherent in the Dynamic Flow Apparatus that Affect the Measurement of Hydrogen Uptake	37
	4.3.3 Repeat Adsorption Measurements on the Same Sample	39
	4.3.4 Repeat Sintering Experiments	40
	4.4 Factors Which Affect Hydrogen Adsorption	40
	4.4.1 Sintering of the Support	41
	4.4.2 Metal-Support Complex Formation	42
	4.4.3 Changes in Crystallite Size	52
	4.4.4 Summary	54
	4.5 The Monometallic Catalysts	55
	4.5.1 Supported Platinum	55
	4.5.2 Supported Iridium	61
	4.5.3 Supported Tungsten	64
	4.6 The Bimetallic Catalysts	64
	4.6.1 Supported Bimetallic Pt/Ir Catalysts	65
	4.6.2 Supported Bimetallic Pt/W Catalysts	79
	4.7 Summary of the Sintering Behaviour of the Catalysts	82
5.	CONCLUSIONS	84
6.	RECOMMENDATIONS	86
REFERENCES		87
APPENDIX A		90
	A-1.1 Introduction	90
	A-1.2 Calibration Of Sample Loop	90

TABLE OF CONTENTS continued

CHAPTER		PAGE
	A-2.1 Dispersion Calculation	97
	A-2.2 Sample Calculation	98
	A-3.1 Suport Surface Area Determination	101
APPENDIX B		105
APPENDIX C		137
	C-1.1 Tungsten Analysis	137
	C-1.2 Reduction of WCl_6 to W In situ	138

LIST OF TABLES

Table	Description	Page
3.1	Relative Uptakes(U/Uo) for the Pt and Ir Catalysts Sintered in Hydrogen	20
3.2	Relative Uptakes(U/Uo) for the Pt and Ir Catalysts Sintered in Oxygen	21
3.3	Relative Uptakes for the Pt and W Catalysts Sintered in Hydrogen	22
3.4	Relative Uptakes(U/Uo) for the Pt and W Catalysts Sintered in Oxygen	23
3.5	The Initial Disperstions of the Catalysts	24
3.6	Variations in the Hydrogen Uptake Between the 1st and 2nd Adsorption	25
3.7	Repeat experiments on Fresh Catalyst Samples	26
3.8	The BET Surface Area Measurements for the Catalyst Support	27
4.1	Relative Intensities of X-ray Diffraction Lines for Catalysts having the same Dispersion and Metal Loading but different Crystallite Size Distributions	45
4.2	Special Sintering Treatments for Pt and Ir Catalysts	48
A-1.1	Calibration of Peak Areas	92
A-1.2	Syringe Calibration	93
A-1.3	Sample Loop Size	94
A-1.4	Sample Loop Calibration	96
A-2.1	Calculation cf Total Pulses Adsorbed for Run #71 from Exp.# 37	99
A-2.2	H/M Values for Exp.# 37	100
B-1	The Hydrogen Chemisorption Data	106

LIST OF TABLES continued

Table	Description	Page
B-2	The Experiments Omitted from the Chemisorption Data in Table B-1	130
B-3	Computer Programs	131
B-3.1	Input Format	131

LIST OF FIGURES

Figure		Page
2.1	The dynamic flow chemisorption apparatus.	10
3.1	X-ray diffraction patterns for fresh 1%Pt/1%W, 1%Pt, 1%Ir and 1%Pt/1%Ir supported on Alon.	28
3.2	X-ray diffraction patterns for 1%Pt/Alon sintered at various conditions.	29
3.3	X-ray diffraction patterns for 1%Ir/Alon sintered at various conditions.	30
3.4	X-ray diffraction patterns for 1%Pt/1%Ir/Alon sintered at various conditions.	31
3.5	X-ray diffraction patterns for 1%Pt/1%W/Alon sintered at various conditions.	32
4.1	Effect of thermal treatment for 1 hour in hydrogen on the normalized uptake for 1%Pt/Alon and 1%Ir/Alon.	56
4.2	Effect of thermal treatment for 16 hours in hydrogen on the normalized uptake of 1%Pt/Alon and 1%Ir/Alon.	57
4.3	Effect of thermal treatment for 1 hour in oxygen on the normalized uptake for 1%Pt/Alon and 1%Ir/Alon.	58
4.4	Effect of thermal treatment for 16 hours in oxygen on the normalized uptake for 1%Pt/Alon and 1%Ir/Alon.	59
4.5	Effect of thermal treatment for 1 hour in hydrogen on the normalized uptake for 1%Pt/1%Ir/Alon and a 50/50 mechanical mixture of 1%Pt/Alon and 1%Ir/Alon.	66
4.6	Effect of thermal treatment for 16 hours in hydrogen on the normalized uptake for 1%Pt/1%Ir/Alon and a 50/50 mixture of 1%Pt/Alon and 1%Ir/Alon.	67

Figure		Page
4.7	Effect of thermal treatment for 1 hour and 16 hours in hydrogen on the normalized uptake for the Platinum and Iridium Catalysts	68
4.8	Effect of thermal treatment for 1 hour in oxygen on the normalized uptake for 1%Pt/1%Ir/Alon and a 50/50 mechanical mixture of 1%Pt/Alon and 1%Ir/Alon.	69
4.9	Effect of thermal treatment for 16 hours in oxygen on the normalized uptake for a 1%Pt/1%Ir/Alon and a 50/50 mechanical mixture of 1%Pt/Alon and 1%Ir/Alon.	70
4.10	Effect of thermal thermal treatment for 1 hour in hydrogen on the normalized uptake for 1%Pt/Alon,1%Pt/1%W/Alon and a 50/50 mechanical mixture of 1%Pt/Alon and 1%W/Alon.	71
4.11	Effect of thermal thermal treatment for 1 hour and 16 hours in hydrogen on the normalized uptake for 1%Pt/Alon and a 50/50 mechanical mixture of 1%Pt/Alon and 1%W/Alon.	72
4.12	Effect of thermal thermal treatment for 1 hour in oxygen on the normalized uptake for 1%Pt/Alon,1%Pt/1%W/Alon and a 50/50 mechanical mixture of 1%Pt/Alon and 1%W/Alon.	73
4.13	The equilibrium phase diagram for Pt-Ir	77

CHAPTER 1

INTRODUCTION

1.1 Supported Metal Catalysts

Supported noble metal catalysts are used in a wide variety of industrially important chemical reactions. Such catalysts consist, in general, of small metal crystallites dispersed over a relatively stable porous material called the support. The metal is the catalytic agent; however, in some cases the support may also participate in the reactions (e.g. the reforming of hydrocarbons). The metal is usually added to the support by immersing the support in an aqueous solution of the metal salt and allowing the water to evaporate. The impregnated salt is then reduced directly to the metal, or calcined in oxygen to form the metal oxide which is then reduced. The resulting metal crystallites may vary in size from >200 nm to smaller than 1 nm. The support is often a metal oxide such as alumina or silica and helps to create and maintain a high metal surface area.

It has been observed for supported metal catalysts that at elevated temperatures and over prolonged periods of time the average metal crystallite size increases. This increase in crystallite size is called sintering and results in a lower metal surface area. Sintering is detrimental to the performance of the catalyst, because the decrease in metal surface area results in fewer 'active' surface sites upon which the catalysed chemical reaction occurs.

In addition to time and temperature, the type of support and the atmosphere above the catalyst have a large effect on the thermal stability of a catalyst, i.e. its resistance to sintering. In certain circumstances the surrounding atmosphere can cause an increase in the metal surface area. This is desireable for the regeneration of deactivated catalysts.

The mechanism by which the crystallites grow is still uncertain. One mechanism considers that the crystallites move across the support surface and then coalesce (1) while another theory suggests that atoms of metal leave one crystallite, travel across the support surface, and then are captured by another crystallite (2). By either theory the fundamental driving force behind the sintering process is the same. This driving force is the reduction in the overall surface free energy of the metal.

1.2 Measurement of Metal Dispersion

There are several different techniques available for measuring the metal surface area of supported metal catalysts (3). Among the simplest is the dynamic flow chemisorption method. In this method a suitable chemisorbing species is chosen. The chemisorbing species should be one that readily bonds to the surface metal atoms (e.g. H_2, O_2, or CO). By measuring the amount of chemisorption and assuming a stoichiometry of the adsorbate to the adsorbent (e.g. 1 H atom adsorbed per 1 Pt surface atom) a metal dispersion can be

determined. The dispersion is defined as the ratio of the number of surface metal atoms to the total number of metal atoms. The dispersion is directly related to the metal surface area, and can be converted to a metal surface area by multiplying the dispersion by the total number of metal atoms and the average area per metal atom.

The various criteria for choosing an adsorbate and the assumptions necessary to calculate the dispersion from adsorption uptakes have been discussed extensively in the literature (4,5,6).

1.3 Supported Bimetallic Catalysts

Supported monometallic catalysts have dominated the industrial scene since the second world war; however, in the past decade bi- and multimetallic catalysts have become widely used. In this case two or more metals are dispersed on the support. The popularity of these catalysts over monometallics is due to several factors. These include:

1. often bimetallics have increased activity thus requiring less severe operating conditions for the catalysed reaction;

2. incorporation of a second metal may lead to different product distributions, i.e. better selectivity;

3. bimetallic catalysts may have increased thermal stability with respect to sintering;

4. bimetallics may retard coke formation (e.g. Pt/Re). (This is of great significance in catalytic reactions

involving hydrocarbons.)

Very little has been published in the open literature on supported bimetallic catalysts especially in regards to the thermal stability. The thermal stability characteristics and other properties of these catalysts depend partly on the surface composition of the metal crystallites. Whereas with monometallic catalysts the composition of the crystallite surface is the same as that of the bulk, this is not necessarily true for the crystallites of bimetallic catalysts. In fact, it is well known that when two or more metals are present as an alloy the surface will be enriched with the metal that has the lower surface energy (or lower heat of sublimation). For bimetallic catalysts it is of interest to know whether the crystallites form alloys or whether the metals remain segregated on the support. Also if alloys are formed, it is of interest to determine the extent to which the surface is enriched with one component and the effect the surrounding environment has on the surface composition.

In the present study the thermal stabilities of the two supported bimetallic catalysts Pt/Ir on alumina and Pt/W on alumina were investigated. There is relatively little in the open literature on the sintering behaviour of either of these two catalysts. This is somewhat surprising since Pt/Ir on alumina is widely used commercially for the reforming of hydrocarbons. It was hoped that through the study of the thermal stability , information could be derived as to the composition of the metal crystallites on the support and the

mechanism (i.e crystallite versus atomic migration) by which the catalysts sinter.

CHAPTER 2

EXPERIMENTAL

2.1 Introduction

This chapter describes the methods for catalyst preparation as well as the procedures used for catalyst characterization. The catalyst preparation is described at some length since this is still very much an art and small variances in procedure can result in quite different dispersion of the metal.

2.2 Catalyst Preparation

Five different catalysts were used in this work: 1%Pt/alumina, 1%Ir/alumina, 1%W/alumina and co-impregnated 1%Pt/1%Ir/alumina, 1%Pt/1%W/alumina. All catalysts were prepared in the laboratory and in all cases the support was Alon. Alon is a commercial gamma-alumina manufactured by the Cabot Corporation of Boston, Massachusetts. The support was impregnated using an agueous solution of the metal salt. Platinum (II) chloride and iridium (III) chloride were purchased from Engelhard Industries of Canada Ltd., Toronto, Ontario. Ammonium metatungstate was obtained from ICN Pharmaceuticals, Plainsview, N.Y.. The analysis of the tungsten content in the metatungstate is outlined in Appendix C.

For the preparation of the monometallic catalysts, a weighed amount of dry Alon (usually 100 grams) was wetted with

distilled de-ionized water until a smooth paste was formed. Approximately 1 ml of water was added per gram of Alon. The required amount of the aqueous salt solution (i.e. that required to give a metal loading of 1 weight percent) was pipetted into a graduated cylinder and diluted with 60 mls of distilled de-ionized water. The contents of the graduated cylinder were slowly added to the alumina paste which was being stirred vigorously. The graduated cylinder was rinsed with several 10 ml portions of distilled de-ionized water and the washings were added to the Alon. The Alon was left to stand for 24 hours, being stirred intermittently. It was then slowly heated, on a hot plate, while being continuously stirred until a thick paste formed. The paste was spread evenly over the walls of the containing vessel (2000 ml beaker) and allowed to air dry for 24 hours. Next, the catalyst was crushed to fine powder and dried in a Fisher Isotemp oven at 110 ^{o}C for another 24 hours.

The procedure for the preparation of the co-impregnated catalysts was the same as that just described for the monometallic catalysts except for one change: the required volumes of the metal salt solutions (plus the 60 mls of distilled de-ionized water) were mixed thoroughly before adding to the alumina paste.

The reduction of the dried catalyst consisted of a series of steps. First the sample was reduced in a flow of hydrogen (50 cc/min) at 150 ^{o}C for 16 hours. The temperature was then increased to 250 ^{o}C for 2 hours and finally 500 ^{o}C for 1 hour.

The sample was purged with nitrogen (50cc/min) and cooled to room temperature. The catalyst was reduced in 20 gram batches and all batches were mixed together to give as homogeneous a catalyst as possible. The reduced catalyst was stored at room temperature in air.

2.3 Experimental Schedule

The objective of the experimental program was to measure the dispersion of the catalysts before and after thermal treatment under a prescribed set of conditions. In all cases the initial dispersion was measured. The initial dispersion will also be referred to as the dispersion of the 'fresh' catalyst or the 'unsintered' catalyst. The catalyst sample was then treated in either hydrogen or oxygen for 1 or 16 hours at a given sintering temperature. The dispersion of the sintered catalyst was measured and a relative uptake (sintered dispersion/ unsintered dispersion) was calculated. The relative uptake was determined over a range of temperatures. The relative uptakes were plotted against temperature to give the sintering curves.

Besides the sintering behaviour of the monometallic and bimetallic catalysts, an investigation of the thermal stability of mechanical mixtures of the Pt and Ir, and, Pt and W monometallic catalyst was made. In this case 50/50 weight percent mixtures were prepared by intimately mixing the catalysts in a mortar with a pestle. The sintering curves for the mechanical mixtures were compared to the curves for the

monometallic as well as the bimetallic catalysts. It was of interest to see if the metals in the mechanical mixtures sintered independently of each other or whether there were synergistic effects due to long range metal transport (e.g. vapour phase transport).

2.4 Dynamic Flow Adsorption Method

The metal dispersion was measured by hydrogen chemisorption. The apparatus used was much the same as that described by Freel (7) and Flynn (8). A schematic diagram of the apparatus is shown in Figure 2.1. Calibration of the apparatus is detailed in Appendix A. The original sample loops on the gas sample valve were too large and a pair of 0.345 cc loops were constructed from 0.125 inch stainless steel tubing.

The initial metal dispersion was measured by the following procedure. An accurately weighed catalyst sample (~1.5 grams for all the platinum and iridium catalysts, ~2.5 grams for the Pt/W bimetallic catalysts and ~3.2 grams for the Pt-W mechanical mixture catalysts) was packed between glass wool in the Vycor U-tube sample holder and purged with hydrogen (50 cc/min). In the later stages of the investigation, sintering was carried out at temperatures >500 °C, and quartz wool instead of glass wool was used. The furnace (Lindberg Box Furnace, Sola Basic Industries Watertown, Wisconsin model 51748) was heated to 500 °C (+/- 2 °C) and controlled using a Thermo Electric

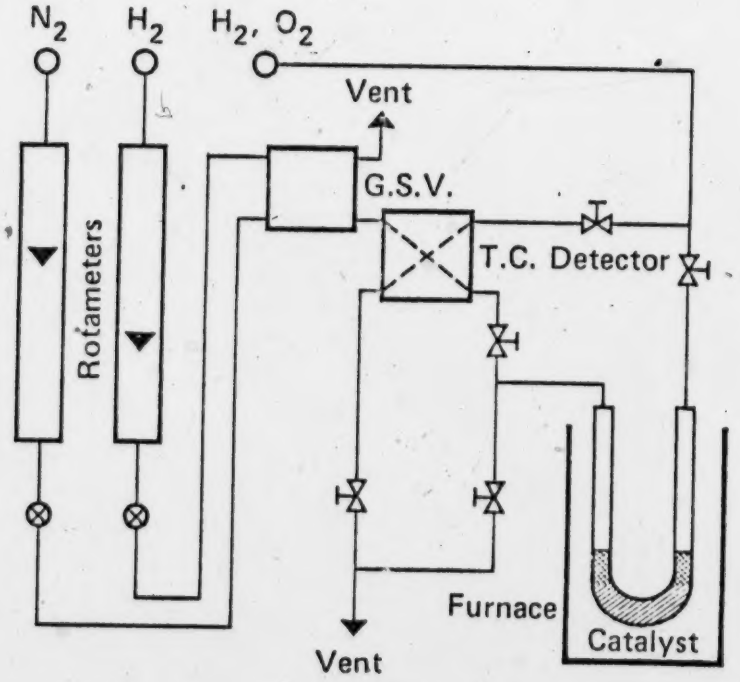

Figure 2.1: The dynamic flow hydrogen chemisorption apparatus

Selectrol temperature controller (Thermo Electric Co. Saddle Brook, N.J. model 381402110). The sample was then placed in the furnace and treated in hydrogen for 1 hour. Hydrogen was used in order to clean the metal surface of any oxides. Next the gas was switched to nitrogen (50 cc/min) and the sample purged for 2 hours. The nitrogen purge allowed for the desorption of hydrogen from the metal surface. The sample holder was removed from the furnace, still purging with nitrogen, and allowed to cool to room temperature. While the sample was cooling the thermal conductivity cell (Gow-Mac Instument Co., Madison, N.J. Model No. 10-735, with rhemium-tungsten filaments, powered by a Gow-Mac Power supply, model 40-05C) was switched on and allowed to warm up. The filament current was preset to 150 mA. The T.C. cell was immersed in an ice water bath. The output from the T.C. cell went to a Hewlett-Packard model 3380A reporting integrator which was also allowed to warm up several minutes prior to use. Hydrogen at a constant flow rate of 50 cc/min was passed through one loop of the 8-port Carle gas sample valve (Carle Instruments Inc., Fullerton, California model 4200.). When the catalyst sample was at room temperature the gas sample valve was electrically activated and injected the volume of hydrogen in the sample loop (0.345 cc) into the nitrogen carrier stream. The gas sample valve had two sample loops and was so designed that when activated one loop which was purging with hydrogen was isolated and flushed with the nitrogen carrier. The other loop which had just previously been flushing with nitrogen was now purged with hydrogen. Pulses

of hydrogen were injected at 3.5 minute intervals until the size of two consecutively eluted peaks, as shown on the integrator, were constant (i.e. no more hydrogen was being adsorbed). The amount of hydrogen adsorbed was calculated as the difference between the amount of hydrogen injected and the amount of hydrogen eluted.

To sinter a sample the furnace was set to the desired temperature. The sample, for which the initial dispersion had just been determined, was purged with nitrogen (50 cc/min) then placed in the furnace and allowed to reach the set temperature. When the set temperature was achieved the nitrogen flow was replaced by the desired gas (flow rate 50 cc/min) in which the sintering characteristics were to be determined. In this study the atmosphere was either oxygen or hydrogen. The sample was allowed to sinter for the required length of time and then the flow was switched back to nitrogen and the sample holder removed from the furnace. The furnace was brought to 500 °C and the same procedure was followed to measure the dispersion of the sintered sample as that used to measure the initial dispersion. In most cases repeat determinations of the hydrogen adsorption were made on the same sample. The procedure for the repeat determinations was to reduce the sample again in hydrogen for 1 hour at 500 °C followed by a 2 hour nitrogen purge. The sample was withdrawn from the furnace, cooled to room temperature, and the hydrogen adsorption uptake was remeasured.

The gases used were of very high purity. Hydrogen was

generated electrolytically with the Matheson Elhygen-R hydrogen generator (Matheson Gas Co. East Rutherford, N.J. model 8320). The hydrogen was further purified to remove traces of oxygen by passing it over an Engelhard Deoxo hydrogen purifier and then over a bed of 4A molecular sieves. The nitrogen was Linde Specialty Gas prepurified (Union Carbide Canada Ltd., Toronto, Ontario). It was further purified to remove traces of oxygen and hydrogen by using a Cu/CuO catalyst heated to 300 °C. The nitrogen was also passed through a bed of 4A molecular sieves. The oxygen was Linde specialty gas, Ultra High Purity, and was used without further purification.

2.5 X-ray Diffraction Measurement

Some of the catalysts used in this study were examined by X-ray diffraction. The diffraction patterns were used qualitatively to examine the changes in the crystallinity of the Alon support and the changes in metal crystallite size due to thermal treatment. The X-ray data was found quite useful in the interpretation of the chemisorption data and the sintering behaviour.

Changes in the crystallinity of the support are important because:

1. Crystallization of the originally amorphous support decreases the surface area which results in metal crystallites becoming inaccessible to the hydrogen adsorbate.

2. Changes in the structure of the support will affect the mobility of the metal and thus affect the rate of sintering.

Metal particle size can be obtained from X-ray diffraction. The presence of small crystalline particles causes a broadening of the diffraction lines. Equations are reported in the literature (9) which relate the line broadening to the average particle size. Although in this work actual particle sizes were not calculated, the X-ray data was used qualitatively to indicate how the metal crystallite size changed with different sintering treatments.

Preparation of the catalyst for an X-ray scan involved crushing the sample to a fine powder. The powder was then lightly sprinkled onto a glass slide which had been coated on one side with petrcleum jelly. The purpose of the jelly was to hold the the powdered sample on the slide. Excess sample was removed from the slide by a gentle tapping. The sample was then mounted in the diffractometer. A Phillips diffractometer (type PW 1380/60 no. 0698) was used. Cu(K_α) (λ=0.1541 nm) radiation was used with a nickel filter. For most of the scans the angle scan rate was 0.125 degrees/min, the attenuation was 4, the CPS was 400 and the time constant 0.4. The scan started at an angle of θ=17 and usually ended at θ=24 if only the changes in the metal crystallite size were being studied. To study changes in the crystallinity of the support the angle was scanned to θ=36.

The diffraction pattern was recorded on a strip chart

with the intensity of signal measured against 2θ. These recordings were traced and replotted versus the d spacings which are obtained by substituting the angle θ into the Bragg equation (10).

2.6 BET Surface Area Measurement

Surface areas of the support were measured by using a standard constant volume BET apparatus. The dead volume determinations were done using helium and the BET isotherms were measured using nitrogen at liquid nitrogen temperatures. The vapour pressure of nitrogen at liquid nitrogen temperatures was measured with a Wallace-Tiernan pressure gauge (Pennwalt, Wallace & Tiernan Division, 1500 Hi Performance Gauge Line, Belleville N.J.). The pretreatment of the catalyst consisted of evacuating the samples at 200 °C to a pressure of $<10^{-3}$ Torr. An average of five points in the range of $0.05 \leq P/Po \leq 0.35$ were measured for each surface area determination. Surface areas of the support were measured for fresh and heavily sintered samples, only, in order to determine the changes of the support area during sintering.

CHAPTER 3

RESULTS

3. Introduction

The hydrogen adsorption results, the X-ray diffraction (XRD) results and the BET surface area measurements are summarized in this section. All the hydrogen adsorption results are listed in Table B-1 of Appendix B. Each experiment in Table B-1 consists of a set of hydrogen chemisorption measurements (called 'runs') for a fresh catalyst sample. The metal dispersions are listed as the 'hydrogen to metal' ratio (H/M) (where H=total atcms of hydrogen adsorbed and M=total metal atoms), and throughout this work the two terms will be used interchangably. The dispersion is equivalent to the H/M only if one H atom chemisorbs on one surface metal atom. There is evidence in the literature (11) that a 1:1 stoichiometry exists for H atoms adsorbed on Pt; however, for Ir and W the adsorption stoichiometry has not yet been established. The presentation of the chemisorption data in terms of the H/M rather than dispersion was perferred, since, the H/M implies no assumptions as to adsorption stoichiometry.

The equation used for calculating H/M is:

$$H/M = \frac{N * V * F * No}{(W/100)*(M1/MW1+M2/MW2)*No} \qquad [3.1]$$

where:

N=the no. of pulses adsorbed (calculated from the peak areas)
V=the average volume of H_2 in the sample loops=0.345 cc.
F=((1/22414)*(2)) moles of H per cc.
No=Avogadro's number

W=the weight of the catalyst sample in grams (a)
M1=the wt.% of metal 1 on the catalyst
M2=the wt.% of metal 2 on the catalyst
MW1=the atomic weight of metal 1
MW2=the atomic weight of metal 2

(a) W=W/2 for the mechanically mixed catalysts

In the case of the bimetallic M in the term H/M represents the total number of metal atoms.

The method used for calculating the H/M and an illustrative example are given in Appendix A. Appendix B lists the computer programs that were written to calculate H/M and tabulate the data as given in Table B-1.

For each experiment listed in Table B-1 a relative uptake was calculated. The relative uptake is the ratio of the average dispersion of the sintered sample to the average dispersion of the unsintered sample. This is equal to the ratio of the amounts of hydrogen adsorbed by the sintered and unsintered sample, thus the term relative uptake.

Relative uptake (RU) is a rather useful concept in the study of chemisorption on supported metal catalysts for several reasons. One reason is that no assumption need be made concerning the adsorption stoichiometry in order to calculate the RU. The only assumption is that the adsorption stoichiometry is independent of the metal crystallite size. A second reason for using relative uptake is to account for inhomogeneities in the metal content and the initial metal dispersion of the catalyst samples. Such inhomogeneities are not only found between different batches of catalyst but also

within the sampling of the same batch. It is found that if two samples from the same batch of catalyst are sintered by exactly the same treatment conditions, the resulting dispersions will be different if the initial dispersions were different. The RU seems to compensate for small variations in the initial dispersion. An example of this is found by comparing the results of Exp.# 37 and Exp.# 38 in Table B-1. In both these sets, a sample of Pt/Ir bimetallic catalyst was sintered in oxygen at 500 °C for 1 hour. The average initial and sintered dispersions for the first set were 0.434 and 0.254 respectively. For the second set the averages were 0.471 and 0.264. Although there is more than an 8% difference between the initial dispersions and a 4% difference between the sintered dispersions, there is only a 2% difference between the relative uptakes. The relative uptake will only 'smooth' the data if the differences in the initial dispersions are small (12). A third reason for using the relative uptake is that systematic errors in the experimental apparatus such as: improperly calibrated sample loops, variations in gas flow rates, temperature and pressure are cancelled. These errors can be significant when calculating the 'absolute' dispersion.

3.2 Adsorption Results

The methods used for sintering the catalysts and measuring the hydrogen adsorption have been discussed previously in the experimental section.

The results from Table B-1 have been summarized in terms of the relative uptake and are listed in Tables 3.1 - 3.4.

Much data were collected on the initial dispersions of the different catalysts. As such an average initial dispersion was calculated for each catalyst. A standard deviation (SD) and the coefficient of varience (CV) were also calculated. The results are given in Table 3.5. The CV is the standard deviation divided by the average (13). Results of repeat uptake measurements on the same catalyst sample are given in Table 3.6. Results of repeat sintering experiments on fresh catalyst samples are given in Table 3.7.

3.3 The BET Surface Area Results

The surface areas of the support were measured for some of the fresh and heavily sintered samples using the BET method. The results are given in Table 3.8. A sample calculation of the surface area is given in Appendix A.

3.4 X-ray Diffraction Results

The X-ray diffraction patterns are shown in Figures 3.1 - 3.5. Intensity of signal is plotted against lattice spacing, d. Increased intensity of the X-ray diffraction lines indicate increased crystallinity.

Table 3.1

Relative Uptakes (H/Ho) for the Pt and Ir Catalysts Sintered in Hydrogen

Sintering Conditions		Relative Hydrogen Uptakes				
Time (h)	Temp. (°C)	1%Pt	1%Ir	1%Pt/1%Ir Bimetallic	1%Pt-1%Ir Physical Mixture	Avg. (a)
1	500(b)	1.00	1.00	1.00	1.00	1.00
	650	0.83 (29) (c)	0.83 (10,11)	0.85 (47)	0.82 (60)	0.83
	800	0.59 (30)	0.76 (12)	0.74 (48)	0.68 (61)	0.68
16	500	1.00	1.00	1.00	1.00	1.00
	650	0.60 (31,32,33)	0.81 (13,14)	0.81 (49)	0.71 (62)	0.71
	800	0.28 (34)	0.62 (15,16)	0.63 (50)	0.51 (63)	0.45

a where: Avg. = (1%Pt+1%Ir)/2
b For all the treatments in hydrogen at 500 the uptake was asumed equal the initial uptake.
c The numbers in the brackets refer to the experiment numbers as given in Table B-1 of Appendix B from which the relative uptakes were obtained.

Table 3.2

Relative Uptakes (U/Uo) for the Pt and Ir Catalysts Sintered in Oxygen

Sintering Conditions		Relative Hydrogen Uptakes				
Time (h)	Temp. (°C)	1%Pt	1%Ir	1%Pt/1%Ir Bimetallic	1%Pt-1%Ir Physical Mixture	Avg. (a)
1	300	0.99 (17,18)	1.18 (1)	1.01 (35)	1.05 (51)	1.09
	400	1.27 (19) (b)	0.83 (2)	0.75 (36)	0.86 (52,53)	1.05
	500	1.52 (20)	0.39 (3)	0.58 (37,38)	1.00 (54)	0.96
	600	0.97 (21)	0.21 (4)	0.60 (39)	0.75 (55)	0.59
	700	0.45 (22)				
16	300	1.05 (23)	1.22 (5)	1.05 (40)	1.07 (56)	1.14
	400	1.22 (24)	0.33 (6)	0.59 (41,42)	0.81 (57)	0.78
	500	2.11 (25)	0.24 (7,8)	0.90 (43,44,45)	1.08 (58)	1.18
	600	1.03 (26)	0.22 (9)	0.52 (46)	0.73 (59)	0.63
	700	0.30 (27)				
	800	0.15 (28)				

a where: Avg. = (1%Pt+1%Ir)/2

b The numbers in the brackets refer to the experiment numbers as given in Table B-1 of Appendix B from which the relative uptakes were obtained.

Table 3.3

Relative Uptakes (U/Uo) for the Pt and W Catalysts Sintered in Hydrogen

Sintering Conditions		Relative Hyrogen Uptakes		
Time (h)	Temp. (°C)	1%Pt	1%Pt/1%W Bimetallic	1%Pt-1%W Physical Mixture
1	500 (a)	1.00	1.00	1.00
	650	0.83 (29) (b)	0.86 (71)	0.62 (79)
	800	0.59 (30)	0.28 (72)	0.51 (80)
16	500	1.00		1.00
	650	0.60 (31,32,33)		0.51 (81)
	800	0.28 (34)		0.28 (82)

a For all the treatments in hydrogen at 500 the uptake was asumed equal the initial uptake.

b The numbers in the brackets refer to the experiment numbers as given in Table B-1 of Appendix B from which the relative uptakes were obtained.

Table 3.4

Relative Uptakes (U/Uo) for the Pt and W Catalysts Sintered in Oxygen

Sintering Conditions		Relative Hyrogen Uptakes		
Time (h)	Temp. (°C)	1%Pt	1%Pt/1%W Bimetallic	1%Pt-1%W Physical Mixture
1	300	0.99 (17,18) (a)		
	400	1.27 (19)	1.09 (64)	0.99 (73)
	500	1.52 (20)	2.02 (65)	1.58 (74)
	600	0.97 (21)	2.58 (66,67)	1.12 (75)
	700	0.45 (22)	1.05 (68)	0.44 (76)
16	300	1.05 (23)		
	400	1.22 (24)		
	500	2.11 (25)		1.09 (77)
	600	1.03 (26)	1.85 (69,70)	
	700	0.30 (27)		
	800	0.15 (28)		

a The numbers in the brackets refer to the experiment numbers as given in Table B-1 of Appendix B from which the relative uptakes were obtained.

Table 3.5

The Initial Dispersions of the Catalysts

Catalyst	# of Independent Measurements	Average Initial H/M	Standard Deviation	% Coefficient of Varience
1%Ir	25	0.443 (0.401-0.482) (a)	0.023	5.3
1%Pt	30	0.409 (0.366-0.461)	0.036	8.8
1%W	no chemisorption			
1%Pt/1%Ir Bimetallic	21	0.429 (0.375-0.472)	0.023	5.3
1%Pt-1%Ir Physical Mix.	23	0.437 (0.390-0.487)	0.024	5.5
1%Pt/1%W Bimetallic	12	0.067 (0.045-0.092)	0.017	24.8
1%Pt-1%W Physical Mix.	13	0.205 (0.184-0.235)	0.017	8.1

a The values in the brackets give the maximum and the minimum H/M obtained for the catalyst.

Table 3.6

Variations in the Hydrogen Uptake
Between the 1st and 2nd Adsorption

Catalyst	Total Pairs of Repeat Adsorptions	% of Adsorption Pairs within 10% (a)	within 5% (b)	% of Adsorption Pairs where the Relative Difference was +'ve and >2.5% (c)	Avg. %CV (d)
1%Pt	28	93	72	75	3.1
1%Ir	25	100	84	90	1.7
1%Pt/1%Ir Bimetallic	19	90	74	86	2.7
1%Pt-1%Ir Physical Mix.	23	91	83	75	2.3
1%Pt/1%W Bimetallic	11	64	27	25	5.8
1%Pt-1%W Physical Mix.	10	90	60	0	3.3

a within 10% = $\left|\frac{(\text{1st adsorption} - \text{2nd adsorption})}{\text{1st adsorption}}\right| \times 100 < 10$

b within 5% = $\left|\frac{(\text{1st adsorption} - \text{2nd adsorption})}{\text{1st adsorption}}\right| \times 100 < 5$

c relative difference = $\left|\frac{(\text{1st adsorption} - \text{2nd adsorption})}{\text{1st adsorption}}\right|$

d The average %CV was calculated from the %CV for each adsorption pair.

Table 3.7

Repeat Experiments on Fresh Catalyst Samples

Catalyst	Exp. #	Treatment atm	°C	h	Relative Uptake U/Uo
Ir	7	OXY	500	16	0.230
	8				0.258
	10	HYD	650	1	0.783
	11				0.883
	13	HYD	650	16	0.821
	14				0.802
	15	HYD	800	16	0.607
	16				0.626
Pt	17	OXY	300	1	0.952
	18				1.027
	31	HYD	650	16	0.621
	32				0.597
	33				0.580
Pt/Ir Bimet	37	OXY	500	1	0.585
	38				0.573
	41	OXY	400	16	0.608
	42				0.565
	43	OXY	500	16	0.889
	44				0.914
	45				0.895
Pt/Ir Mix	52	OXY	400	1	0.862
	53				0.847
Pt/W Bimet	66	OXY	600	1	2.544
	67				2.623
	69	OXY	600	16	1.710
	70				1.982

Table 3.8

The BET Surface Area Measurements for the Catalyst Support

Cat.	Exp. #	Treatment Atm	Temp (°C)	Time (h)	Surface Area sq. m/g
1%Pt		unsintered			96.4
	22	OXY	700	1	96.7
1%Ir		unsintered			95.5, 96.0
	12	HYD	800	1	94.1
	16	HYD	800	16	93.2
1%W		unsintered			102.3
1%Pt/1%Ir Bimet.		unsintered			96.4
	50	OXY	800	16	92.4
1%Pt/1%W Bimet.		unsintered			96.0
	68	OXY	700	1	100.8
	69	OXY	600	16	101.6
	71	HYD	650	1	95.1
	72	HYD	800	1	97.8

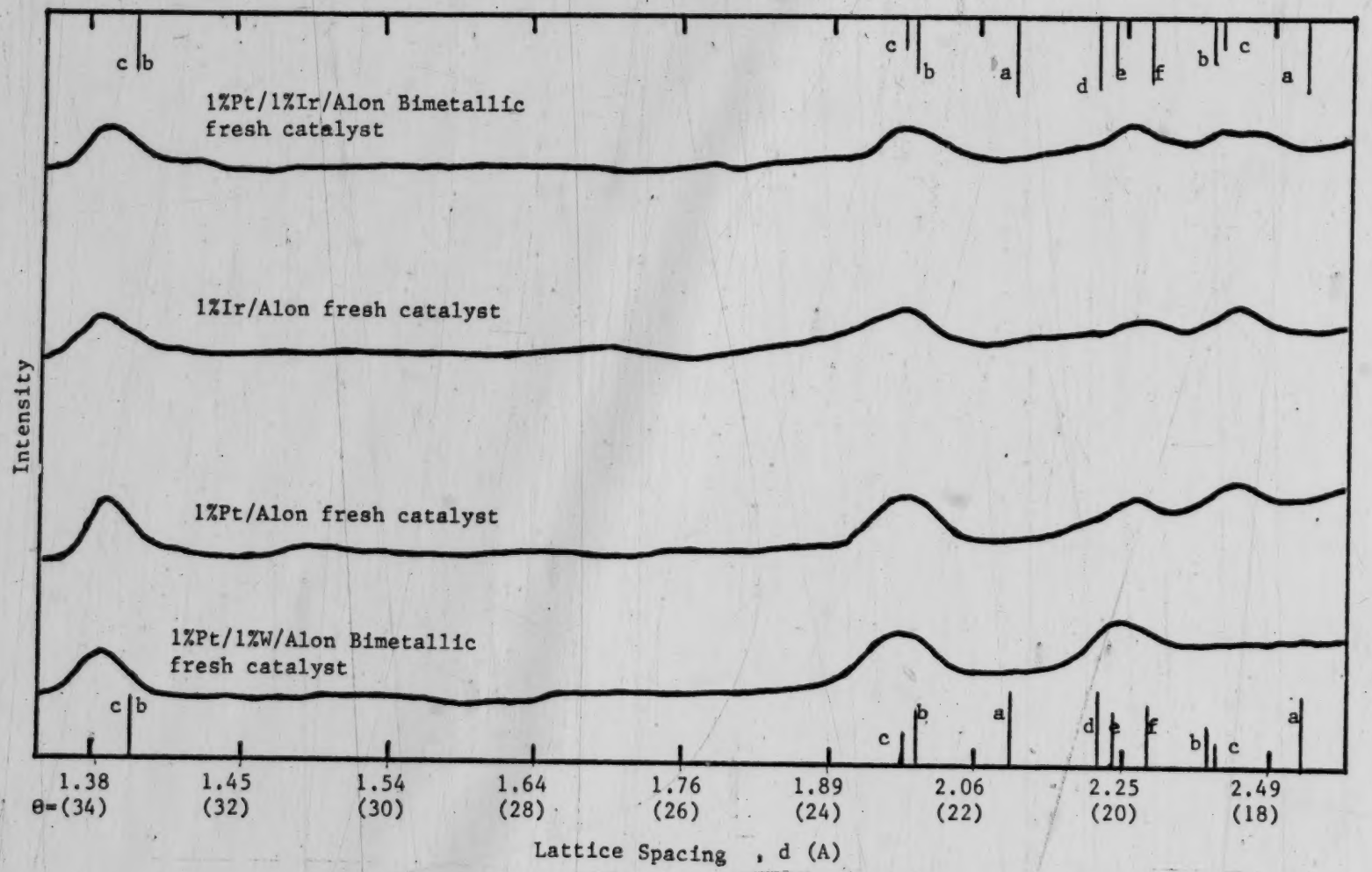

Figure 3.1: X-ray diffraction patterns for unsintered 1%Pt/1%W, 1%Pt, 1%Ir and 1%Pt/1%Ir/ supported on Alon. (Lines indicated correspond to a=α-Al_2O_3 ; b= γ-Al_2O_3 , c= η-Al_2O_3 , d=Ir, e=W, f=Pt)

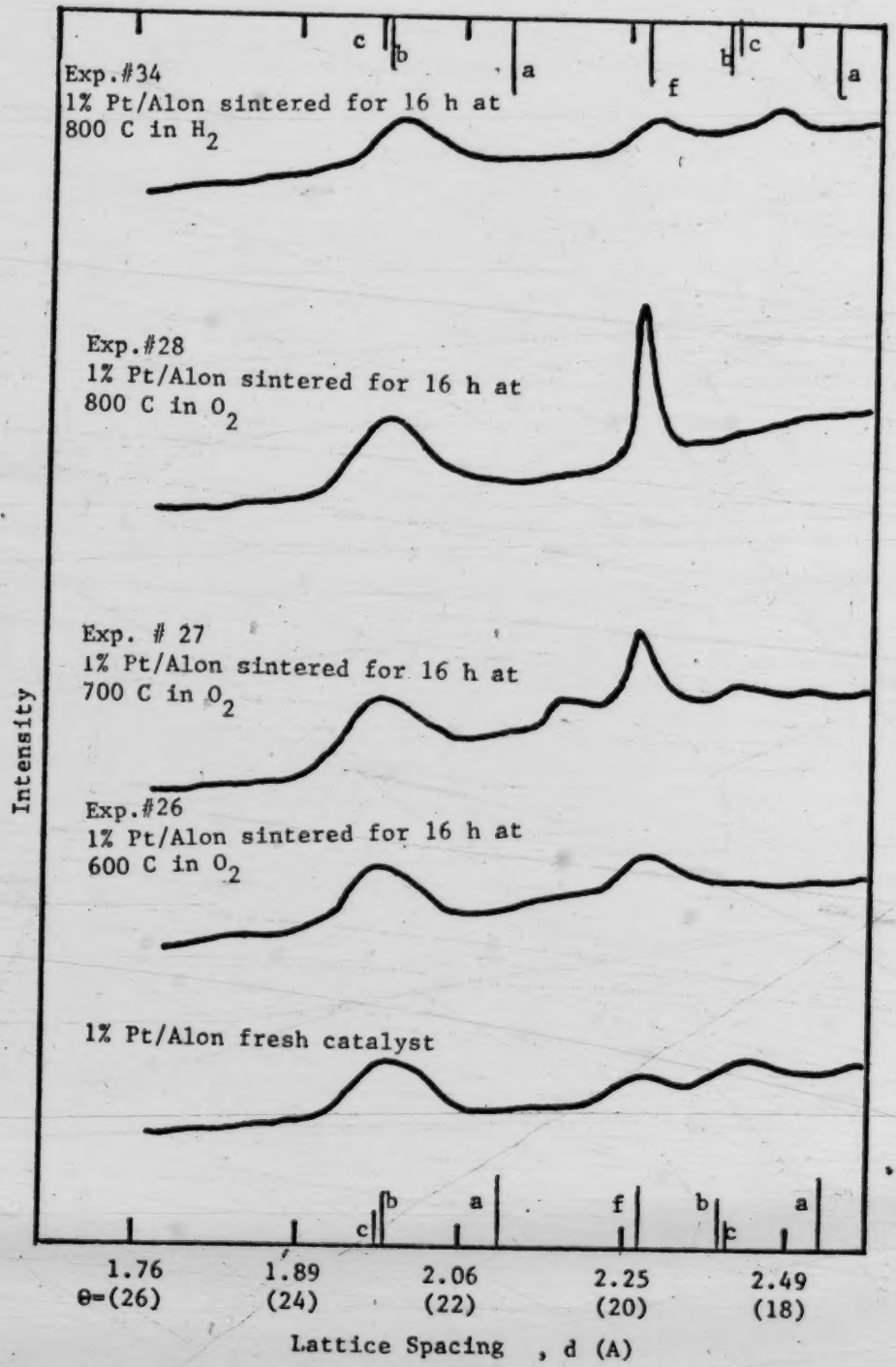

Figure 3.2: X-ray diffraction patterns for 1%Pt/Alon sintered at various conditions. (Lines indicated correspond to: a=α- Al_2O_3 , b= γ- Al_2O_3 , c= η- Al_2O_3 , f=Pt)

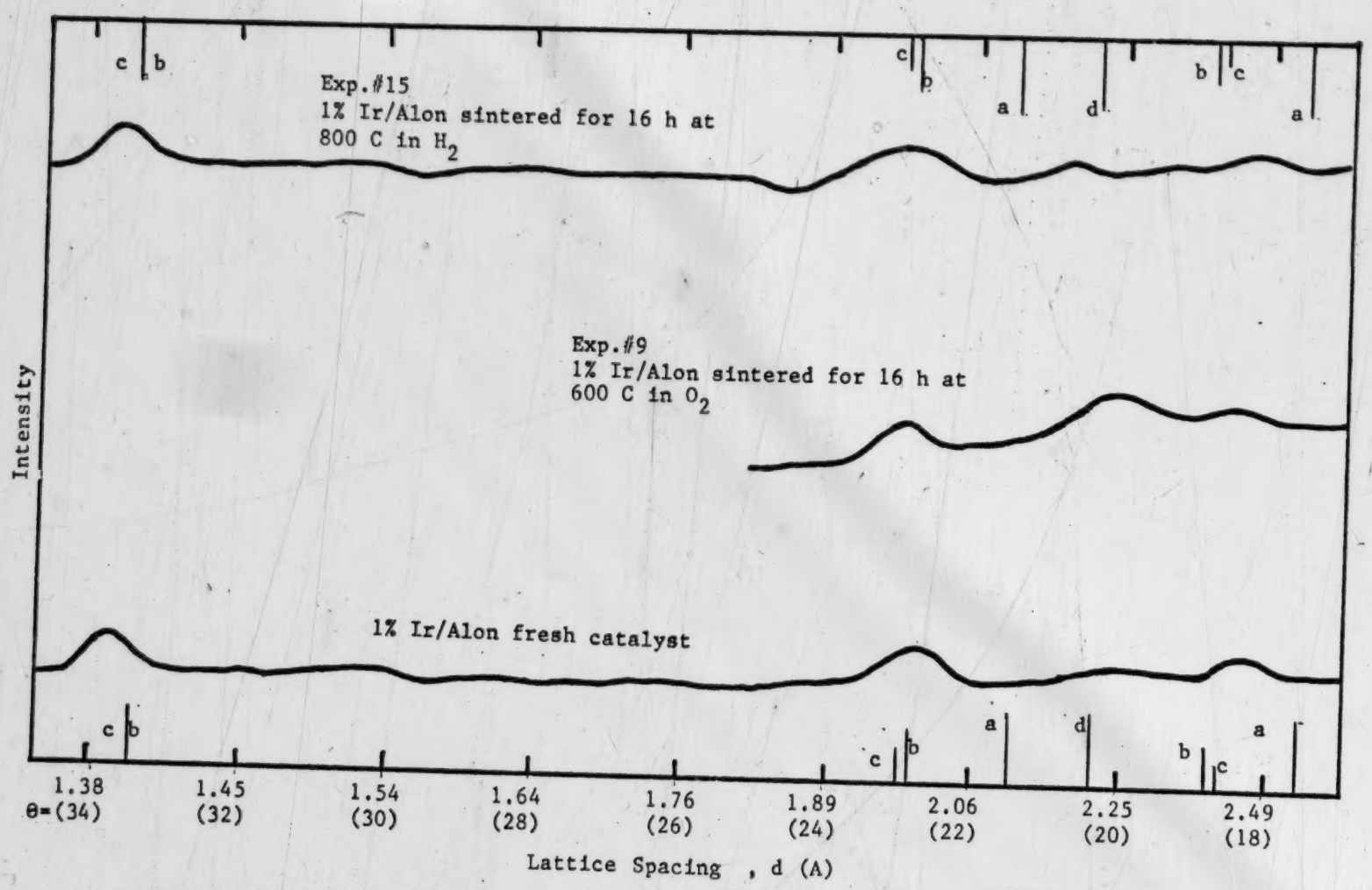

Figure 3.3: X-ray diffraction patterns for 1%Ir/Alon sintered at various conditions. (Lines indicated correspond to: a=κ-Al_2O_3, b=γ-Al_2O_3, c=η-Al_2O_3, d=Ir)

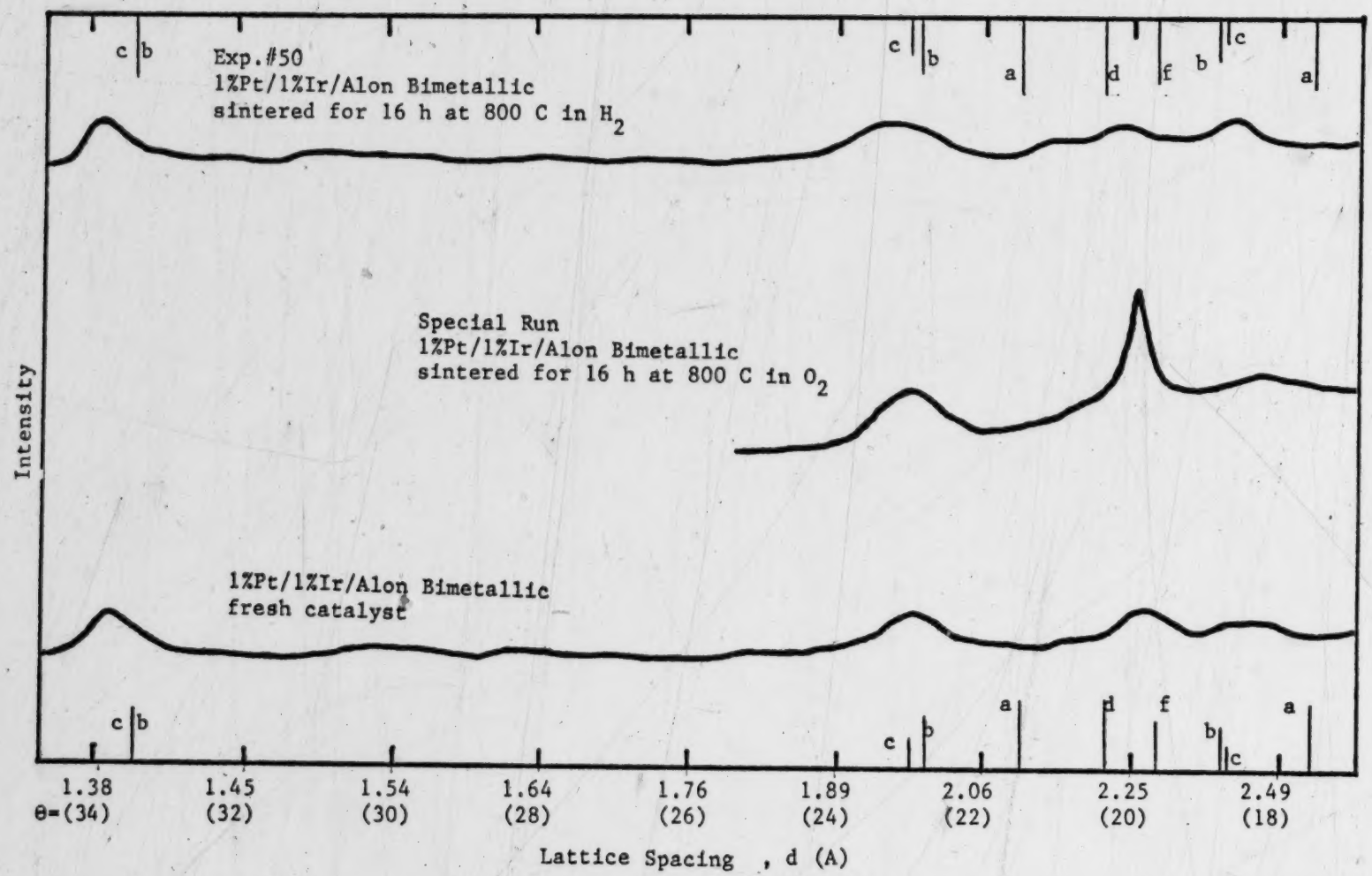
Exp.#50
1%Pt/1%Ir/Alon Bimetallic
sintered for 16 h at 800 C in H_2
Special Run
1%Pt/1%Ir/Alon Bimetallic
sintered for 16 h at 800 C in O_2
1%Pt/1%Ir/Alon Bimetallic
fresh catalyst
Intensity
1.38 1.45 1.54 1.64 1.76 1.89 2.06 2.25 2.49
θ=(34) (32) (30) (28) (26) (24) (22) (20) (18)
Lattice Spacing , d (A)

Figure 3.4: X-ray diffraction patterns for 1%Pt/1%Ir/Alon sintered at various conditions. (Lines indicated correspond to: a=α-Al_2O_3, b=γ-Al_2O_3, c=η-Al_2O_3, f=Pt, d=Ir)

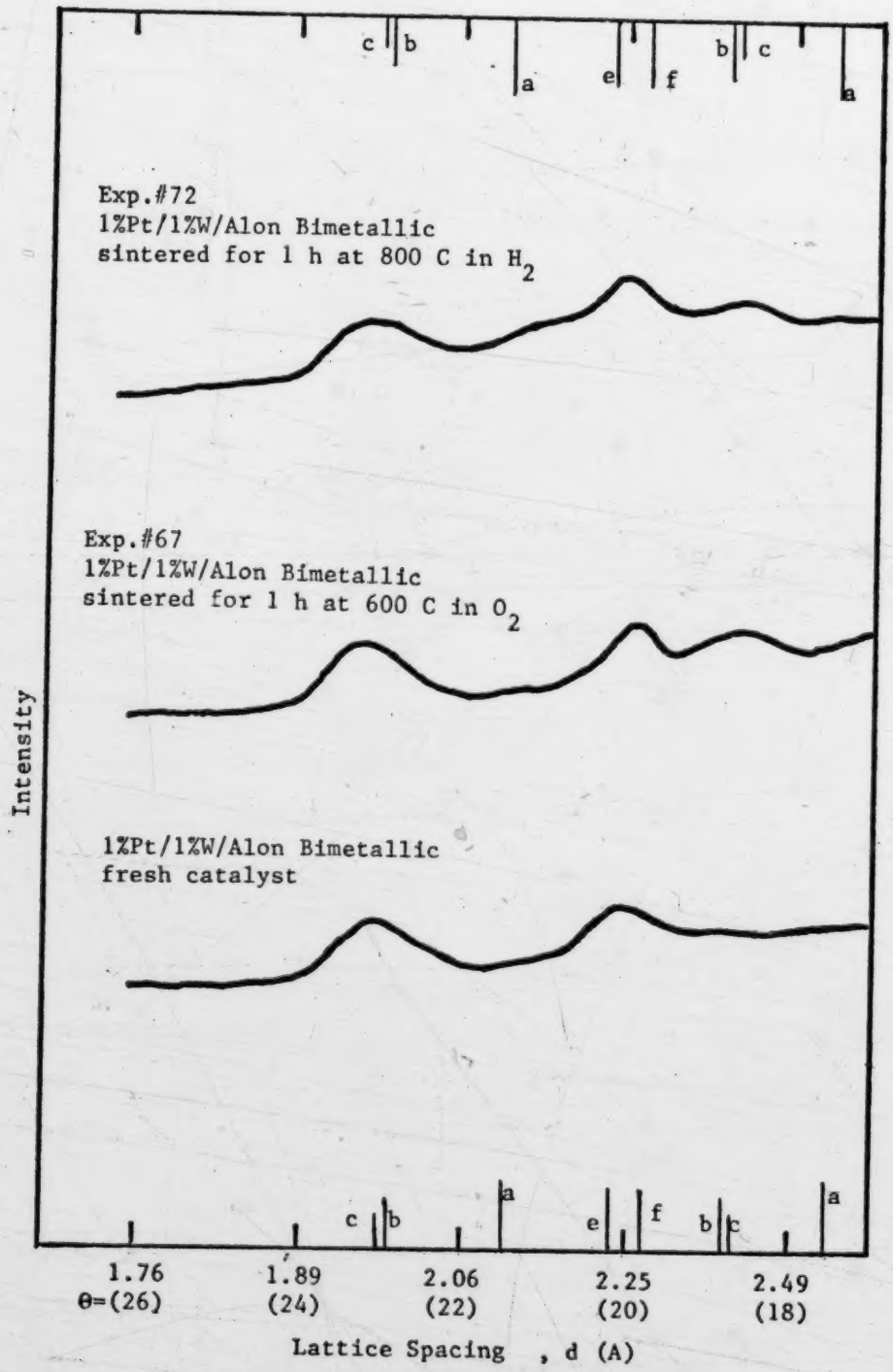

Figure 3.5: X-ray diffraction patterns for 1%Pt/1%W/Alon sintered at various conditions. (Lines indicated correspond to: a=α-Al_2O_3, b=γ-Al_2O_3, c=η-Al_2O_3, e=W, f=Pt)

Chapter 4

DISCUSSION

4.1 Introduction

The topics discussed in this chapter are:

1. the factors which affect initial metal dispersion on the support;

2. the limitations of the dynamic flow technique and the repeatability of hydrogen chemisorption measurements;

3. the factors that affect hydrogen adsorption on the catalyst;

4. the results of the sintering experiments for the monometallic Pt, Ir and W catalysts and the bimetallic Pt/Ir and the bimetallic Pt/W catalysts.

4.2 Factors Affecting Initial Metal Dispersion

In order to make a meaningful comparison between the thermal stabilities of the different supported metal catalysts, the catalysts have to have approximately the same initial metal dispersion (12). An even metal distribution on the support is also desired. Achievement of these properties is dependent on a number of factors, the first being, the method of addition of the metal to the support. In this study the impregnation technique was used because of its simplicity. Other factors considered during the preparation of the

catalysts are discussed in the rest of this section.

4.2.1 Choice of Metal Salt

Consideration was given to the type of metal salt to be used for the impregnation of the support. The criteria for choosing the salt included such things as: the solubility in water; the rate of adsorption on the support and the ease of reduction in hydrogen.

Since aqueous solutions of platinum and iridium chloride had worked well for others (14,15) these salts were used for the preparation of the monometallic catalysts. For the bimetallic Pt/Ir catalyst adaptations of the preparation techniques of McKee and Norton (16) and others (17) were used. It was decided that a mixture of aqueous solutions of platinum and iridium chlorides would be suitable. The use of ammonium metatungstate for the monometallic W and the Pt/W bimetallic catalysts was suggested by Mertzweiller (18).

4.2.2 Choice of Support

The use of Alon as the support helped in the preparation of a well dispersed metal. Alon is a fumed γ-alumina with an average particle size in the range of 30 nm. The use of Alon allowed for rapid and thorough mixing of the support with the metal salt solution. The use of non-porous Alon also circumvented the problems of uneven metal distribution due to pore diffusion which is common with pellets (19).

4.2.3 Choice of Reduction Treatment

The catalysts were reduced for 16 h in hydrogen at 150 °C. The low temperature reduction promoted the formation of a highly dispersed metal on the support. To ensure that all of the metal salt had been reduced the catalysts were further treated in hydrogen for 1 h at 250 °C and 1 h in hydrogen at 500 °C.

To further increase the homogeneity of the catalyst batch, the catalyst was crushed to a fine powder and mixed thoroughly.

4.2.4 Summary

The experimental procedures outlined in the experimental section were strictly followed so as to ensure a uniform preparation of the catalysts thus reducing, to a minimum, any variation in the catalysts due to preparation technique. Unfortunately the following of any catalyst receipe as closely as possible cannot ensure the preparation of a uniformly dispersed metal. There are too many possible sources of variation. For example, it was found in this study that the rate of drying of the impregnated catalyst was very critical. The first batch of Pt catalyst prepared had a crust of yellow platinum chloride on the catalyst paste surface. It was evident that too rapid drying had leached out the platinum salt. Subsequently the drying procedure was changed to involve a slow heating of the catalyst while it was being constantly stirred. At the point when the catalyst paste was

quite thick, it was spread over the walls of the containing vessel and allowed to air dry for 24 h. This technique stopped the 'leaching' problem.

Table 3.5 gives the initial dispersions for the catalysts. It is seen from the table that for the monometallic Pt and Ir and the Pt/Ir bimetallic catalysts some success was achieved in preparing catalysts with approximately the same initial dispersion. The initial dispersions for the set of platinum and iridium catalysts were all within 10% of each other. The 1%Pt/Alon catalyst had the largest CV (8.8%) for the set. The other platinum and iridium catalysts had CV's typically around 5.3%. The initial dispersion of the Pt/W bimetallic catalyst was quite low (0.067) and the CV was high (24%). This was likely due to the chemical system rather than the preparation technique. To illustrate how the initial metal dispersion varied through the batches of catalysts, Table 3.5 gives the range found in the measurement of the initial dispersion.

4.3 Hydrogen Chemisorption Measurement

4.3.1 The Dynamic Flow Method

A dynamic flow method similar to that described by Flynn (8) was used to measure hydrogen chemisorption. Hydrogen pulses were injected into the nitrogen carrier stream which passed through the catalyst bed. By measuring the amount of hydrogen injected to the catalyst and the amount of hydrogen

eluted from the catalyst, the hydrogen uptake of the catalyst was calculated. It was assumed that the hydrogen uptake was due, primarily, to rapid and irreversible hydrogen chemisorption on the surface of the metal crystallites. There were other possible sources of hydrogen adsorption which may have contributed to the measured uptake. These other sources include spillover of hydrogen to the support and hydrogen dissolution into the metal crystallites (20).

The great advantage of the dynamic flow method is its simplicity of design and its rapidity in measuring hydrogen chemisorption. The biggest disadvantage of the method is that it only measures hydrogen adsorption which is rapid and irreversible. As such, the measured adsorption is generally lower than that found by the 'static' adsorption method (21).

4.3.2 Factors Inherent in the Dynamic Flow Apparatus that Affect the Measurement of Hydrogen Uptake

Variations in the measured hydrogen uptake for a catalyst can be attributed to several variable factors inherent in the experimental apparatus. These variable factors include: the amount of hydrogen injected per pulse; the catalyst sample size and nitrogen flow rate; the time between pulse injections and the carrier gas purity.

Differences in the pulse size can arise from changes in the atmospheric temperature and pressure, improper port alignment in the gas sample valve and changes in the hydrogen flow rate. Since the atmospheric pressure and temperature

changes were usually small (i.e. < 10 mmHg and < 2 °C) these fluctuations account for only a 1 or 2 % change in the amount of hydrogen in the pulse. Improper port alignment however is a more serious problem. If the ports are not aligned exactly, the restriction in the hydrogen flow through the sample loops could result in an increased hydrogen pressure in the loops and thus more hydrogen injected per pulse. Serious port misalignment was not observed. The flow rate of hydrogen was always maintained at 50 cc/min and only small fluctuations were observed in the flow.

All the hydrogen chemisorbed on the metal surface was not irreversibly adsorbed. It was found for 1 gram of either the Pt or Ir monometallic catalyst, 7.2% of a pulse of hydrogen was lost when the catalyst was purged for 15 min in nitrogen at room temperature. The time between hydrogen injections was therefore a factor in the total measured amount of hydrogen uptake. Because a variation in the time between pulse injections could change the measured amount of hydrogen adsorbed, a fairly constant period of 3.5 min between pulse injections was used.

As mentioned in the experimental section, precautions were taken to rid the carrier gas of traces of oxygen and hydrogen. Small traces of these contaminants can seriously affect the amount of hydrogen adsorbed on the catalyst. For example consider a case where 1.5 g of 1%Pt catalyst, with an initial dispersion of 0.402, is purged with nitrogen, containing 10 ppm of oxygen, for 2 hours at a 50

cc(STP)/min flow rate. Assuming that all the oxygen is chemisorbed by the platinum during the nitrogen purge, 35% more hydrogen will be required in the uptake measurement than if no oxygen was present in the nitrogen. The extra hydrogen adsorption is due to the hydrogen reacting with the chemisorbed oxygen (to produce water). Small quantities of oxygen in the nitrogen carrier gas can therefore have a very large effect on the measured uptake.

4.3.3 Repeat Adsorption Measurements on the Same Sample

For a catalyst sample the hydrogen uptake was generally measured twice and the repeatability of the adsorption measurements is shown in Table 3.6. (To perform the second adsorption measurement, the chemisorbed hydrogen from the first measurement was removed by purging the catalyst for 2 hours at 500 ^{o}C with nitrogen.) From Table 3.6 it is seen that in a majority of cases the second uptake measurement was within 10% of the first uptake measurement and except for the bimetallic Pt/W catalyst, the second uptake was generally within 5% of the first uptake. In a majority of cases, for both the fresh and sintered Pt and Ir catalysts the second hydrogen uptake measurement was less than the first hydrogen uptake measurement. For the preparation of the table it was somewhat arbitrarily chosen that repeat uptakes within 2.5% of each other would be assumed equal. Differences in the hydrogen adsorption between the first and second uptake measurements has been observed by others (14); however no suitable explanation of the cause of this difference has ever

been given. In the case of the Pt/W bimetallic and the Pt-W mechanically mixed catalysts, the second hydrogen uptake was generally larger than the first.

4.3.4 Repeat Sintering Experiments

To test the repeatability of the sintering experiments several repeat experiments were carried out on fresh catalyst samples. These results are shown in Table 3.7. Overall the repeatability was quite good. Most of the repeat determinations lay within 10% of each other. A coefficient of variance (CV) was calculated for each of the repeat determinations and an overall average CV was calculated for all of the results in Table 3.6. The overall average CV was 4.2%. The repeat experiments showed that the techniques used to sinter the catalysts and the methods of measuring the hydrogen chemisorption gave repeatable results.

4.4 Factors Which Affect Hydrogen Adsorption

Changes were observed in the amount of hydrogen chemisorbed by the catalysts. The reasons for the change in uptake included: catalyst inhomogenity; variations in experimental procedure; changes in the support area and support crystallinity; metal-support surface reaction; variation in the average metal crystallite size.

The causes of catalyst inhomogenity and variations inherent in the experimental procedure were discussed in the first two sections of this chapter. This section will discuss the remaining three.

4.4.1 Sintering of the Support

At high temperatures many catalyst support materials decrease in surface area. The reasons for the decrease are: collapse of the pore structure; increased crystallinity of the support and possible agglomeration of the support particles. In all cases the decrease in the surface area can result in the entrappment of the metal. The metal thus becomes inaccessible to the chemisorbing gases and so the hydrogen uptake decreases.

The Alon support used in this study was non-porous. There was little loss in surface area even after severe treatment (heating at 800 °C for 16 h). Table 3.8 shows that with the exception of the 1%W catalyst, the initial support surface area of the fresh catalysts was approximately 96 m^2/g. The theoretical surface area calculated for spherical particles of Alon 30 nm in diameter is ~50 m^2/g. Non-sphericity and surface roughness of the Alon particles accounts for the measured surface area being larger than the theoretical surface area. Treating the different catalysts under a variety of conditions resulted in a surface area change of only a few square meters per gram. No correction for the change in support area was made to the dispersions given in Table B-1. The support area for the tungsten catalysts seemed to be somewhat higher than the support areas measured for the Pt and Ir catalysts. This may have been due to the surface complex formation between the W and the alumina support (discussed later).

An increase in the crystallinity of the support can also result in metal crystallites becoming inaccessible to the chemisorbing gas. The X-ray data shown in Figures 3.1 - 3.5 shows no substantial changes in the crystallinity of the support. This is indicated by the lack of an increased intensity of the alumina diffraction lines.

4.4.2 Metal-Support Complex Formation

Low hydrogen uptakes would also result, if the metal reacted with the support to give a non-hydrogen adsorbing surface complex. Such complexes have been postulated for both W and Pt on alumina.

4.4.2.(a) Tungsten-Alumina Complex

The 1%W/Alon catalyst prepared by the impregnation of the Alon with ammonium metatungstate could neither be reduced to metallic tungsten nor was there any hydrogen adsorption on the catalyst. As Biloen and Pott (23) found, WO_3 when deposited on γ-alumina and calcined, reacted to form an irreducable tungsten compound. They postulated the formation of a surface tungstate $Al_2(WO_4)_3$. The structure of the complex is undoubtedly similar to the surface structure given by Massoth (24) for the reaction of MoO_3 with γ-alumina. Accordingly the WO_3 / γ-alumina complex would be:

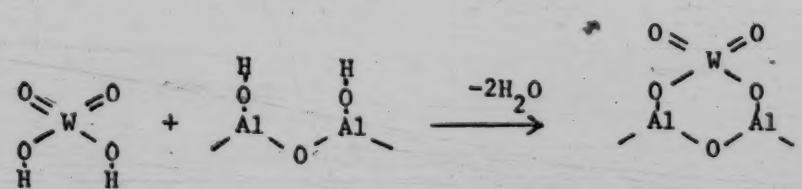

(4.1)

The formation of an irreducible complex of tungsten on alumina was also found by Sondag and co-workers (25). Sondag observed that tungsten could be reduced to the metallic state but the reduction depended strongly on the type of alumina used and the concentration of the W on the support.

4.4.2(b) Pt/Al_2O_3 & Ir/Al_2O_3 Surface Complex

The possibility of a reaction between Pt and alumina was suggested by Sprys and Mencik(26) from their electron microscopy studies.

Recently Dautzenberg and Wolters (27) found that after treating a Pt/Al_2O_3 catalyst in hydrogen at temperatures >500 °C the H/Pt decreased yet X-ray diffraction and electron microscopy studies showed no appreciable increase in the average Pt crystallite size. They proposed a reaction:

$$Pt + Al_2O_3 + xH_2 \longrightarrow Pt{\cdot}Al_2O_{3-x} + x\,H_2O \qquad (4.2)$$

where $Pt{\cdot}Al_2O_{3-x}$ does not adsorb hydrogen. They suggested that the formation of $Pt{\cdot}Al_2O_{3-x}$ results in lower H/Pt without an increase in the average Pt crystallite size. Their sintering studies in oxygen gave lower H/Pt along with increased Pt crystallite size. No surface complex was postulated for the sintering in oxygen.

The X-ray diffraction data shown in Figure 3.2 would tend to verify the findings of Dautzenberg and Wolters. A

crystalline Pt peak of increasing intensity appeared when the Pt catalyst was sintered at temperatures >600 °C in oxygen. The Pt peak indicates the formation of large crystallites. The X-ray pattern for the catalyst sintered in hydrogen at 800 °C for 16 h shows no appreciable change in the Pt crystallinity but there is a substantial decrease in the hydrogen uptake. Although the decrease in H/M could be due to the formation of $Pt{\cdot}Al_2O_{3-x}$, the low uptake of hydrogen and the lack of increase in the intensity of the Pt X-ray diffraction lines may also be explained as follows. If in the sintering of a fresh catalyst, the crystallites grow to form larger crystallites all with approximately the same size (i.e. a 'narrow' particle size distribution) the dispersion can be significantly lower than the dispersion for the fresh catalyst with no observable change in the intensity of the X-ray diffraction lines. Table 4.1 illustrates this point. The table gives the variation in crystallite size and relative X-ray diffraction line intensity for several different dispersions of a hypothetical Pt catalyst. The 'INITIAL' catalyst is composed of 800 spherical Pt particles with an initial dispersion of 0.41. Distribution number 1a, although for a hypothetical catalyst, represents what may happen to a real Pt catalyst when sintered in hydrogen. In 1a pairs of the initial 800 Pt particles have coalesced to form 400 particles 3.15 nm in diameter. The dispersion has decreased from the INITIAL 0.41 to 0.32. Changes such as these can readily be detected by chemisorption techniques. The X-ray line intensity has doubled; however, this increase may not be

Table 4.1

Relative Intensities of X-ray Diffraction Lines for Catalysts having the Same Dispersion and Metal Loading but different Crystallite Size Distributions

Distribution Number	Fraction of Metal with Unity Dispersion(a)	Crystallites(b) size (nm)	Number	Dispersion	Relative X-ray Diffraction Line Intensity(c)
INITIAL	0	2.50	800	0.41	1.0
1 a	0	3.15	400	0.32	2.0
b	0.160	5.26	72	0.32	7.8
c	0.202	7.09	28	0.32	18.2
d	0.289	20.72	1	0.32	400.7
2 a	0	3.97	200	0.26	4.0
b	0.083	5.42	72	0.26	9.3
c	0.176	10.10	10	0.26	54.3
d	0.209	21.46	1	0.25	500.7
3 a	0	6.30	50	0.16	16.0
b	0.0511	8.40	20	0.17	36.0
c	0.0718	10.18	11	0.16	62.7
d	0.1070	22.35	1	0.15	638.0

a Part of the metal goes to form a number of crystallites all the same size. A fraction of the metal with unity dispersion is required in order to give the required dispersion.

b The size and number of crystallites are based on a fixed amount of Pt.

c The intensity of the diffracted beam for small crystals is proportional to the square of the number of unit cells in the crystal (56). Since the number of unit cells in a crystal is proportional to the volume of the crystal, the intensity of the diffracted beam is proportional to the diameter raised to the sixth power.

readily observable. This is due to a number of factors including: the amount of metal loading on the catalyst; instrument background noise; the type of diffractometer used and the X-ray diffraction techniques employed. Thus case 1a is an example where a substantial decrease in the dispersion occurs without an observable increase in the Pt crystallinity. Where increased Pt crystallinity is indicated by increased X-ray line intensity. Distribution 1d represents what may happen to a real Pt catalyst when sintered in oxygen. Here part of the initial 800 Pt particles have formed 1 large crystallite 20.7 nm in diameter with a fraction of the metal, 28.9%, dispersed as Pt atoms so as to give the same dispersion as in 1a. In this case however the X-ray diffraction line intensity is 400.7 times that for the INITIAL case. Case 1d is an example where decreases in dispersion may be followed by increased X-ray diffraction line intensity. The other cases presented in Table 4.1 further illustrate the point that large variations in X-ray intensity can occur for catalysts having the same metal loading and dispersion, but different crystallite size distributions.

The diffraction data for the iridium catalyst in Figure 3.3 and the X-ray data of Chahar (28) for iridium on alumina show qualitatively the same results as those just discussed for Pt. As such an iridium surface complex, $Ir \cdot Al_2O_{3-x}$, could be postulated to explain the low hydrogen uptake and the lack of detection of large crystallites when the catalyst is sintered at high temperatures in hydrogen. As in the case of Pt, the surface complex formation is not necessarily needed to

explain the results.

The X-ray diffraction data for the Pt/Ir bimetallic catalyst is given in Figure 3.4. As one might expect the same qualitative differences in the diffraction patterns after sintering in oxygen and hydrogen were observed as those observed for the Pt and the Ir catalysts.

The X-ray diffraction data for the bimetallic Pt/W catalyst is given in Figure 3.5. In this case no large Pt crystallite formation was indicated after the catalyst was sintered in hydrogen for 1 h at 800 °C. The relative uptake for the catalyst was low (RU=0.28). Again it is possible to postulate a surface complex formed between the Pt and the alumina support. For the bimetallic Pt/W catalyst sintered in oxygen at 600 °C for 1 h, the X-ray data showed no appreciable decrease in dispersion nor any appreciable increase in dispersion. The hydrogen uptake measurements did indicate, however, a large redispersion of the metal.

In order to investigate the possible formation of the $Pt{\cdot}Al_2O_{3-x}$ complex a series of experiments were carried out. These experiments are outlined in Table 4.2. Dautzenberg and Wolters proposed that the $Pt{\cdot}Al_2O_{3-x}$ surface compound would be sensitive to oxygen in that:

$$Pt{\cdot}Al_2O_{3-x} + (1/2)xO_2 \longrightarrow Pt + Al_2O_3 \qquad (4.3)$$

Therefore treating a previously reduced Pt/Al_2O_3 catalyst

Table 4.2

Special Sintering Treatments for Pt and Ir Catalysts

Run #	Treatment	H/M
283	The initial dispersion was measured on a fresh Ir catalyst sample using the normal procedure.	0.467
284	A repeat adsorption measurement on the Ir sample in run 283.	0.451
285	The iridium catalyst was sintered in oxygen for 16 h at 300°C. It was then reduced in hydrogen at 300°C for 1 h and then purged with nitrogen at 300°C for 2 h and 2 more h at 500°C.	0.590
286	Repeat adsorption measurement on run 285 with just a 2 h nitrogen purge at 500°C.	0.543
289	The initial dispersion was measured for a fresh Ir catalyst sample using the normal procedure.	0.424
290	A repeat of the adsorption measurement of run 289.	0.413
291	The Ir sample was sintered in hydrogen for 16 h at 650°C.	0.308
292	The Ir sample from run 291 was sintered in oxygen for 1 h at 300°C. It was then reduced in hydrogen for 1 h at 300°C and then purged with nitrogen for 2 h at 500°C.	0.456
293	The sample from 292 was treated for 1 h in hydrogen at 500°C and then purged with nitrogen for 2 h at 500°C.	0.239
294	The sample in 293 was purged with nitrogen for 2 h at 500°C.	0.235
295	The initial dispersion was measured on a fresh Pt catalyst using the normal procedure.	0.413
296	A repeat adsorption on run 295 was made.	0.399

Table 4.2 cont'd

Run #	Treatment	H/M
297	The Pt sample was sintered in oxygen for 16 h at 400 °C. It was then reduced in hydrogen for 1 h at 400 °C followed by a 1 1/2 h nitrogen purge at 400 °C and a 1 h nitrogen purge at 500 °C.	0.523
298	A repeat uptake measurement was done by purging the sample in run 298 with nitrogen for 2 h at 500 °C.	0.513
299	The sample in run 298 was reduced in hydrogen at 500 °C for 1 h and then purged for 2 h with nitrogen at 500 °C.	0.454

in oxygen should increase the measured H/Pt. They observed that the H/Pt for a catalyst treated in hydrogen could be returned to almost the same H/Pt for the fresh catalyst after 5 oxidation/reduction treatment cycles. Our oxidation results were somewhat inconclusive. Runs 295-299 in Table 4.2 outline an experiment where a sample of the 1%Pt/Alon catalyst was pretreated in the normal fashion in hydrogen at 500 °C and then treated in oxygen at 400 °C for 16 h. The catalyst was reduced at 400 °C for 1 h and then purged with nitrogen. It was thought that the oxygen treatment followed by the low temperature reduction would result in the generation of more available Pt metal for hydrogen chemisorption. The relative uptake of 1.27 was comparable to the relative uptake of 1.22 found using the normal treatment methods. No large increase in the H/Pt was observed. There was a 12% drop in the uptake after the sample was treated for 1 h in hydrogen at 500 °C. This may have indicated $Pt{\cdot}Al_2O_{3-x}$ formation; however this decrease may also be attributed to the normal decrease (although somewhat high) observed for the second hydrogen adsorption measurement. The lack of increase in H/Pt after the low temperature oxidation indicates that either there was no formation of $Pt{\cdot}Al_2O_{3-x}$ or reaction (4.3) did not proceed to an appreciable exent under the conditions of the oxidation treatment. Runs 283-286 in Table 4.2 outline a series of similar experiments for the Ir catalyst. The oxidation temperature had to be even lower than that used in the Pt experiments in order to avoid the complication of heavily sintering the Ir. In this case the RU under the special

treatment (at 300 °C for 16 h in oxygen) was 1.23 compared to a RU of 1.22 under normal treatment conditions. Again there is no indication of formation of a surface complex. Runs 289-294 showed a 48% increase in the H/Ir for a sample treated in oxygen at 300 °C for 1 h which had been previously treated in hydrogen at 650 °C for 16 h. Assuming that the percent redispersion of the Ir catalyst from run 291 would be about the same as that for a fresh catalyst treated in oxygen for 1 h at 300 °C, the 48% increase is significant (i.e. compared to the 18% increase normally observed - see exp. 1 Table B-1). It was also observed that when the sample was reduced in hydrogen at 500 °C for 1 h the uptake dropped by 48%. The results from runs 289-294 tend to support the existence of reactions (4.2) and (4.3) for Ir. This conclusion differs from the conclusions drawn from the other runs in Table 4.2. As such the results of runs 289 - 294 appear to be anomalous and repeat experiments should be done.

In summary the X-ray diffraction data for the Pt catalyst sintered in oxygen and sintered in hydrogen confirm the X-ray findings of Dautzenberg and Wolters. Similar results were found for the Ir catalyst and the Pt/Ir bimetallic catalyst. The chemisorption experiments were inconclusive in proving or disproving the theory of a surface reaction between Pt or Ir and alumina. It was found that a more conventional explanation could explain the X-ray and chemisorption data without the need for a non-hydrogen adsorbing surface complex.

4.4.3 Changes in Crystallite Size

The usual cause of decreased hydrogen adsorption is metal sintering. As the metal crystallites increase in size more and more metal becomes incorporated into the bulk of the crystal leaving smaller numbers of metal atoms exposed at the surface.

Essentially two mechanisms have been proposed to explain how the crystallites actually grow. Both theories are based on the same driving force, that is, the reduction of the overall surface free energy.

One mechanism proposed by Ruckenstein and Pulvermacher (28) suggests that the crystallites travel over the surface of the support and coalesce to form large crystallites. This mechanism predicts a sintering rate law of the form:

$$-\frac{dS}{dt} = K_s S^n \qquad [4.1]$$

where:

S=metal surface area

t=time

Ks=experimental constant

n=exponent

The value of n lies between 2 and 8 depending on whether the rate of fusion (particle sintering) or the rate of surface diffusion is rate controlling. The limitations of the model are that exponent values outside the 2 and 8 have been observed (29). Also this model does not explain redispersion

of the metal.

Another mechanism proposed by Flynn and Wanke (2), suggests that atoms leave the surface of one crystallite, travel across the surface of the support and are captured by another crystallite. Their rate equation is based on the continuity equation:

net growth of a particle =
rate of gain of atoms on the surface - [4.2]
rate of loss of atoms on the surface

The rate of loss of metal atoms is dependent on the energy barrier for an atom to cross from the crystal surface to the support surface. The rate of gain of metal depends on a sticking coefficient, the number of migrating metal species on the surface and the diameter of the crystallite. The advantage of the Flynn and Wanke model is that it predicts values of exponent in equation [4.1] outside the 2-8 range. It also predicts the possibilty of metal redispersion and also allows for the interactions due to the support and the atmosphere in the rate of sintering.

Wynblatt and Gjostein (30) have derived a set of their own equations that not only account for surface diffusion but also for vapour phase transport.

4.4.4 Summary

It has been stated that lower hydrogen uptake can occur due to:

1. entrapment of metal particles due to support sintering and/or support crystallization;

2. formation of a surface complex which makes the metal inaccessible to hydrogen;

3. increased average crystallite size.

From the BET measurements it was found that the Alon surface area changed only slightly even after treatment at 800 °C for 16 h. The X-ray diffraction data showed that there was no observable change in the support crystallinity.

Impregnation of Alon with ammonium metatungstate resulted in the formation of a irreducible, non-hydrogen adsorbing surface complex. The surface complex is thought to be $Al_2(WO_4)_3$. The X-ray data for the platinum, iridium and bimetallic Pt/Ir catalysts sintered in oxygen, show the formation of large crystallites at increased sintering temperatures. The X-ray data for catalysts sintered in hydrogen showed no formation of large crystallites ever after sintering at 800 °C for 16 h. The X-ray diffraction data did not unambiguously prove the existence of a Pt or Ir surface complex as suggested by Dautzenberg and Wolters. A series of special sintering experiments were inconclusive in demonstrating the existence of these surface complexes.

It is believed that the main cause of reduced hydrogen uptake in the sintering experiments was due to an increase in the average metal crystallite size. Most likely the sintering occurs by the atomic migration model.

4.5 The Monometallic Catalysts

The thermal stabilities of monometallic 1%Pt, 1%Ir and 1%W on Alon were investigated for two reasons. The first was so a comparison could be made between the thermal stabilities of the monometallic catalysts and the thermal stabilities of the bimetallic and mechanical mixtures, and second, very little has been published on the thermal stabilities of these monometallic catalysts. (A good deal has been published for Pt however not using Alon as a support.)

The sintering curves for the monometallic Pt and Ir catalysts are given in Figures 4.1-4.4. The relative or 'normalized' uptakes were plotted as a function of the sintering time and the sintering temperature for each of the sintering atmospheres. The data for the plots were taken from Tables 3.1 and 3.2. Note that there was no observable hydrogen adsorption on the W catalyst.

4.5.1 Supported Platinum

The thermal stability of 1%Pt/Alon in hydrogen is given in Figures 4.1 and 4.2. The figures show that the hydrogen uptake decreased monotonically with sintering time and sintering temperature. As a comparison, the relative

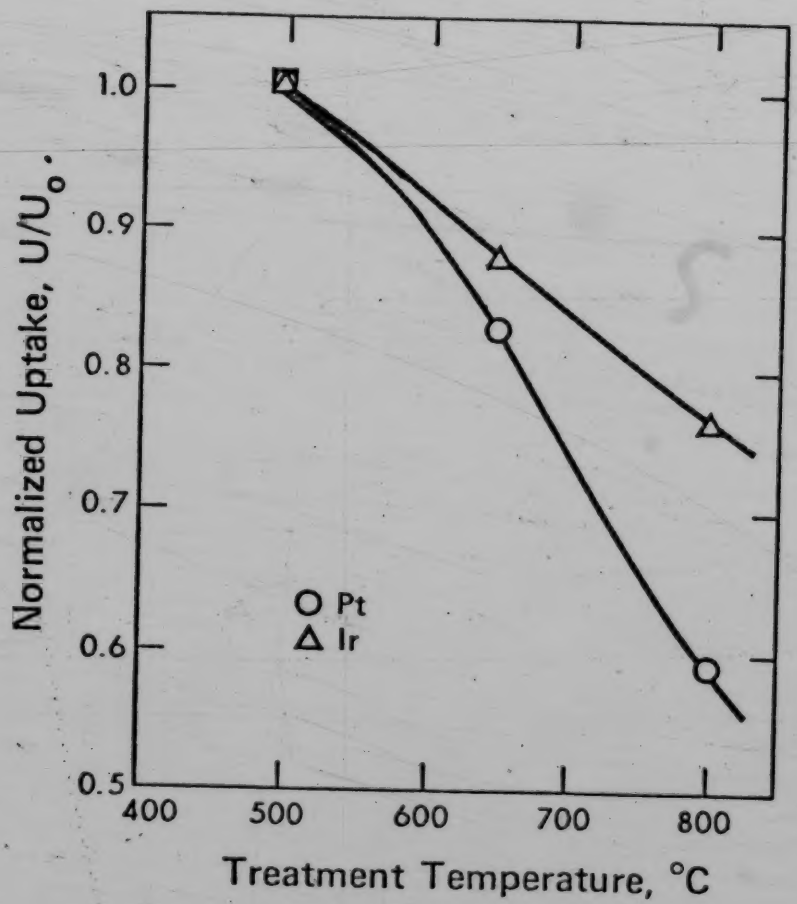

Figure 4.1: Effect of thermal treatment for 1 h in hydrogen on the normalized uptake for 1%Pt/Alon and 1%Ir/Alon

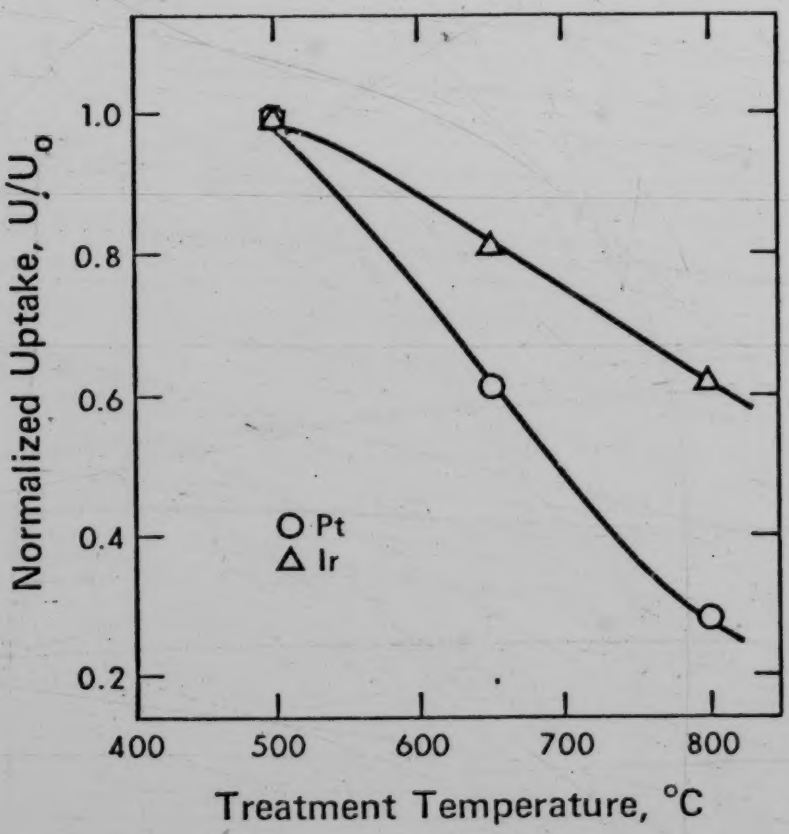

Figure 4.2: Effect of thermal treatment for 16 h in hydrogen on the normalized uptake for 1%Pt/Alon and 1%Ir/Alon

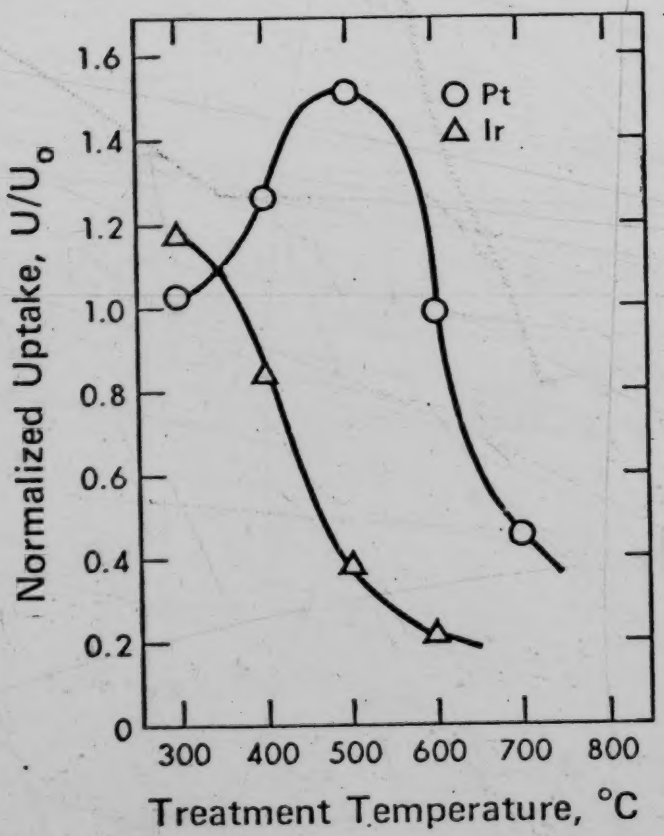

Figure 4.3: Effect of thermal treatment for 1 h in oxygen on the normalized uptake for 1%Pt/Alon and 1%Ir/Alon

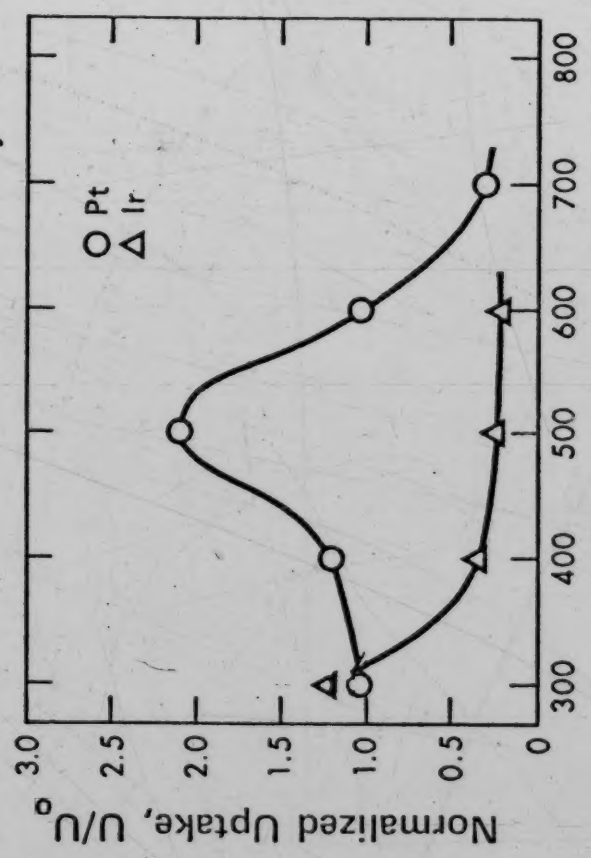

Figure 4.4: Effect of thermal treatment for 16 h in oxygen on the normalized uptake for 1%Pt/Alon and 1%Ir/Alon

uptake was 0.83 and 0.59 at 650 and 800 °C respectively after 1 h sintering. After 16 h the uptakes at 650 and 800 °C were 0.60 and 0.28. The decreases in RU are attributed to a reduction in the metal surface area.

The thermal stability of 1%Pt/Alon in oxygen is shown in Figures 4.3 and 4.4. The stability of Pt in oxygen is much less than the stability in hydrogen. It was found that at temperatures >600 °C the relative uptake rapidly decreased. This decrease, increased with sintering time and temperature. It was also observed for the Pt catalyst that between 400 and 600 °C a RU > 1.00 occured. This is attributed to a redispersion of the metal. A maximum RU of 2.11 was observed after sintering the catalyst in oxygen for 16 h at 500 °C.

Similar results for the sintering of Pt on alumina have been found by others (14,15,31). Chahar (32) in his studies with 2%Pt/Kaiser alumina and Engelhard commmercial 0.5%Pt/alumina catalyst found somewhat greater stability of Pt in hydrogen and somewhat less redispersion in oxygen. Chahar found a maximum redispersion in oxygen at 550 °C and little difference in the amount of redispersion after 1, 4 and 16 h. Differences between Chahar's results and those for the 1%Pt/Alon can be attributed to the use of different alumina supports; different initial metal dispersions and metal loadings; and slightly different methods used for sintering the catalysts.

Fiedorow and Wanke (14) have also reported the redispersion of supported Pt in oxygen. They explain the

redispersion in terms of atomic migration on the support. According to the theory, in the initial stages of sintering a number of migrating surface species (possibly PtO_2) accumulate on the support. If, during this time of enhanced migration the catalyst is cocled, the surface species remain as small clusters and the total metal surface area is increased. Fiedorow and Wanke suggest that at temperatures <600 °C migrating oxide species are formed while at temperatures above 600 °C the oxide decomposes into Pt and oxygen gas. The Pt atoms are highly mobile and are captured by the large crystallites. This explains the rapid sintering of Pt in oxygen at temperatures >600 °C.

In hydrogen the sintering of the metal is the result of simple atom transport (perhaps as Pt-H) across the support.

4.5.2 Supported Iridium

The thermal stability of 1%Ir/Alon in hydrogen is shown in Figures 4.1 and 4.2. The curves are similar to those for Pt except, as the figures show, Ir is more thermally stable than Pt, especially at 800 °C. The sintering curves for Ir in oxygen are given in Figures 4.3 and 4.4. Some redispersion of the Ir occured at 300 °C (18% increase after 1 h and a 22% increase H/M after 16 h); however at higher temeperatures the Ir sintered very rapidly. After treatment at 500 and 600 °C the metal had lost most of its surface area. Ir was much less thermally stable in oxygen than Pt.

The findings cf Chahar (27) for the thermal stability of

Ir/alumina catalysts were somewhat different than the findings presented here for 1%Ir/Alon. Chahar found greater thermal stability in hydrogen for 2%Ir/Kaiser alumina. In oxygen, Chahar found a maximum redispersion of 18% occured at 400 °C after 1 h. For longer sintering times at 400 °C the dispersion decreased markedly. Chahar also noticed quite a rapid drop in the the dispersion at temperatures >500 °C. The variations between Chahar's results and the results for the 1%Ir/Alon were likely due to the different supports, the different initial metal dispersions and metal loadings and differences in experimental technique.

An explanation of the increased thermal stability in hydrogen of Ir compared to Pt can be found using the atomic migration theory. In order for surface metal atoms to jump from the surface of the crystal to the support they must cross an energy barrier at the crystallite surface. The required energy will be proportional to the heat of sublimation (assuming that interactions between the metal and the support and between the metal and the hydrogen environment have roughly the same effect on the heats of sublimation for Pt and Ir). The heats of sublimation for Ir and Pt are 692 and 511 kJ/mole respectively (33). Thus the increased thermal stability of Ir can be correlated to its higher heat of sublimation. Correlations between the heat of sublimation and metal thermal stability in hydrogen have been reported by others (34).

The sintering mechanism for Ir in oxygen is likely

similar to that for Pt. A mobile iridium oxide species that decomposes to the metal plus oxygen gas, at temperatures > 500 °C, could account for the redispersion and the rapid sintering. Enhanced sintering rates of Ir compared to Pt in oxygen may also have been due to vapour phase transport of the Ir as a volatile oxide. Evidence of vapour phase transport lies in the fact that the vapour pressure of iridium oxides are relatively high (35). Also it was observed that when a sample of 1%Ir/Alon was sintered in oxygen at 800 °C for 16 h, a black film was deposited on the walls of the sample holder just outside the furnace. This film was believed to be IrO_2.

Wynblatt and Gjostein (34) have correlated the thermal stability of several metals including Pt and Ir in oxygen, to the heats of formation of the metal oxides. They state that the increased exothermicity of metal oxide formation correlates to decreased thermal stability. It can be concluded in this case that the sintering of the metals is by metal oxide species.

McVicker et al. (36) have recently studied the redispersion of iridium on alumina in oxygen. For a 1%Ir/alumina catalyst they found an initial H/M ratio in excess of 1. They attributed this to hydrogen spillover and/or the possiblity of multiple hydrogen bonding of hydrogen on the corner and edge atoms. McVicker et al. found that Ir dispersion rapidly decreased with length of sintering time. McVicker et al. sintered the catalysts at temperatures greater than 500 °C and did not observe any redispersion.

4.5.3 Supported Tungsten

It was thought that the more refractory nature of tungsten and its high heat of sublimation (846 kJ/mole (33)) would produce a supported catalyst with even greater thermal stability in hydrogen than that for Ir. Ammonium metatungstate was used to impregnate the catalyst but, it was found that upon reduction of the impregnated catalyst, a surface complex formed which was irreducible in hydrogen and did not adsorb hydrogen. The catalyst was prepared by the standard techniques to ensure consistency in preparation.

4.6 The Bimetallic Catalysts

There are several features of bimetallic catalysts which make them harder to prepare and harder to characterize. First, impregnating the support with different metal salts can result in uneven metal distribution, especially if one metal ion is more strongly adsorbed by the support than the other (19,37,38). Second, the metals may form alloyed crystallites or the metals may remain segregated on the support surface. Third, an immiscibility gap can result in formation of metal crystallites with varying compositions. Fourth, there can be enrichment of one metal at the surface of the crystallite due to differences in the surface free energy of the metals. Fifth, the surface composition of the crystallite can also depend on the surrounding environment including interaction with the support and the atmosphere.

In this section the thermal stability of bimetallic

1%Pt/1%Ir and bimetallic 1%Pt/1%W supported on Alon is discussed.

An insight into the composition of the metal crystallites and the reasons for their sintering behaviour was gained by comparing the thermal stabilities of the monometallic and mechanical mixtures of the monometallic catalysts with the thermal stabilities of the bimetallic catalysts.

The thermal stability curves for bimetallic Pt/Ir and bimetallic Pt/W supported on Alon are given in Figures 4.5-4.12. The thermal stabilities of 50/50 wt.% mixtures of the monometallic catalysts are also given in the figures as well as the arithmetic average of the Pt and Ir sintering curves (i.e. (Pt+Ir)/2). The relative uptake was plotted as a function of the sintering time and sintering temperature for each of the sintering atmospheres. The relative uptake data for the figures were taken from Tables 3.1-3.4.

4.6.1 Supported Bimetallic Pt/Ir Catalysts

The thermal stabilities of the bimetallic Pt/Ir catalyst and the mechanical mixtures of Pt and Ir monometallic catalysts in hydrogen are shown in Figures 4.5 and 4.6. The thermal stability for both catalysts decreased monotonically with increased sintering temperature and increased sintering time.

It was found that the thermal stability of the bimetallic Pt/Ir catalyst was essentially the same as the thermal

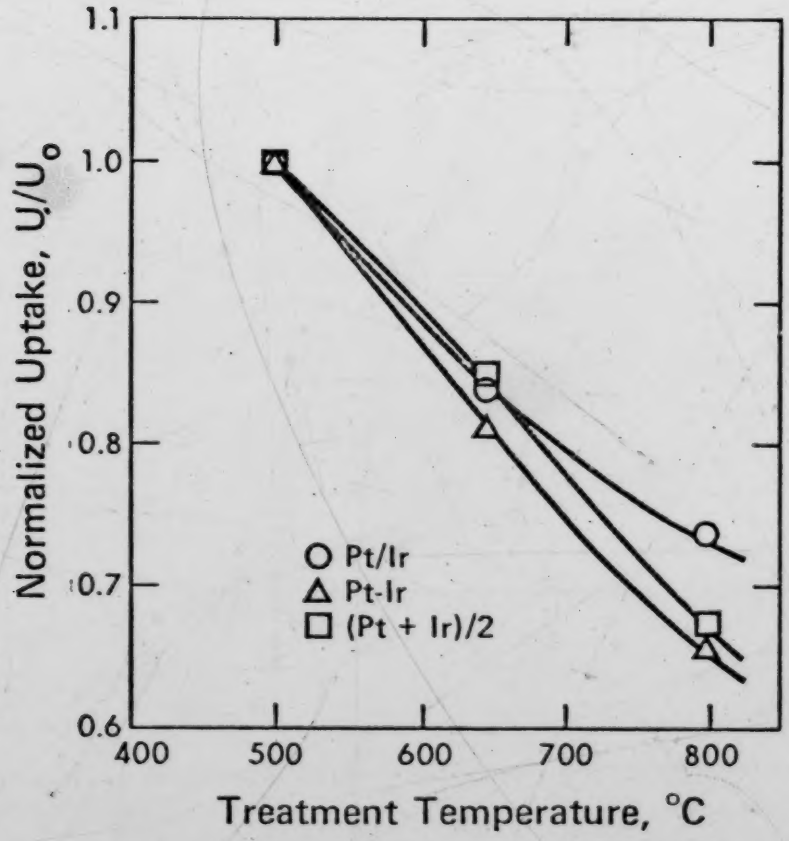

Figure 4.5: Effect of thermal treatment for 1 h in hydrogen on the normalized uptake for 1%Pt/1%Ir/Alon and a 50/50 mechanical mixture of 1%Pt/Alon and 1%Ir/Alon.

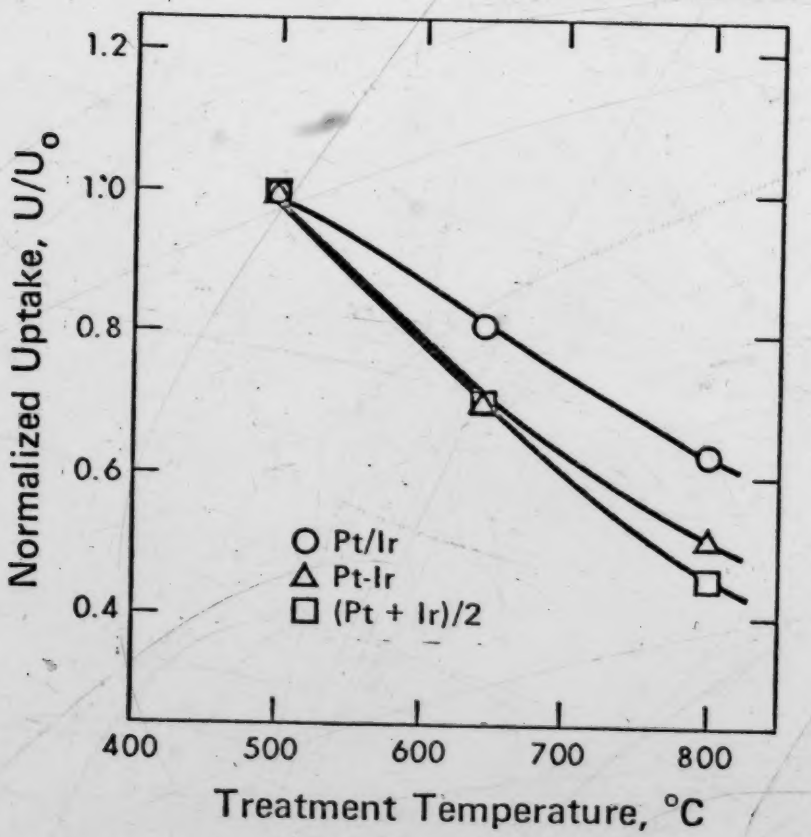

Figure 4.6: Effect of thermal treatment for 16 h in hydrogen on the normalized uptake for 1%Pt/1%Ir/Alon and a 50/50 mechanical mixture of 1%Pt/Alon and 1%Ir/Alon.

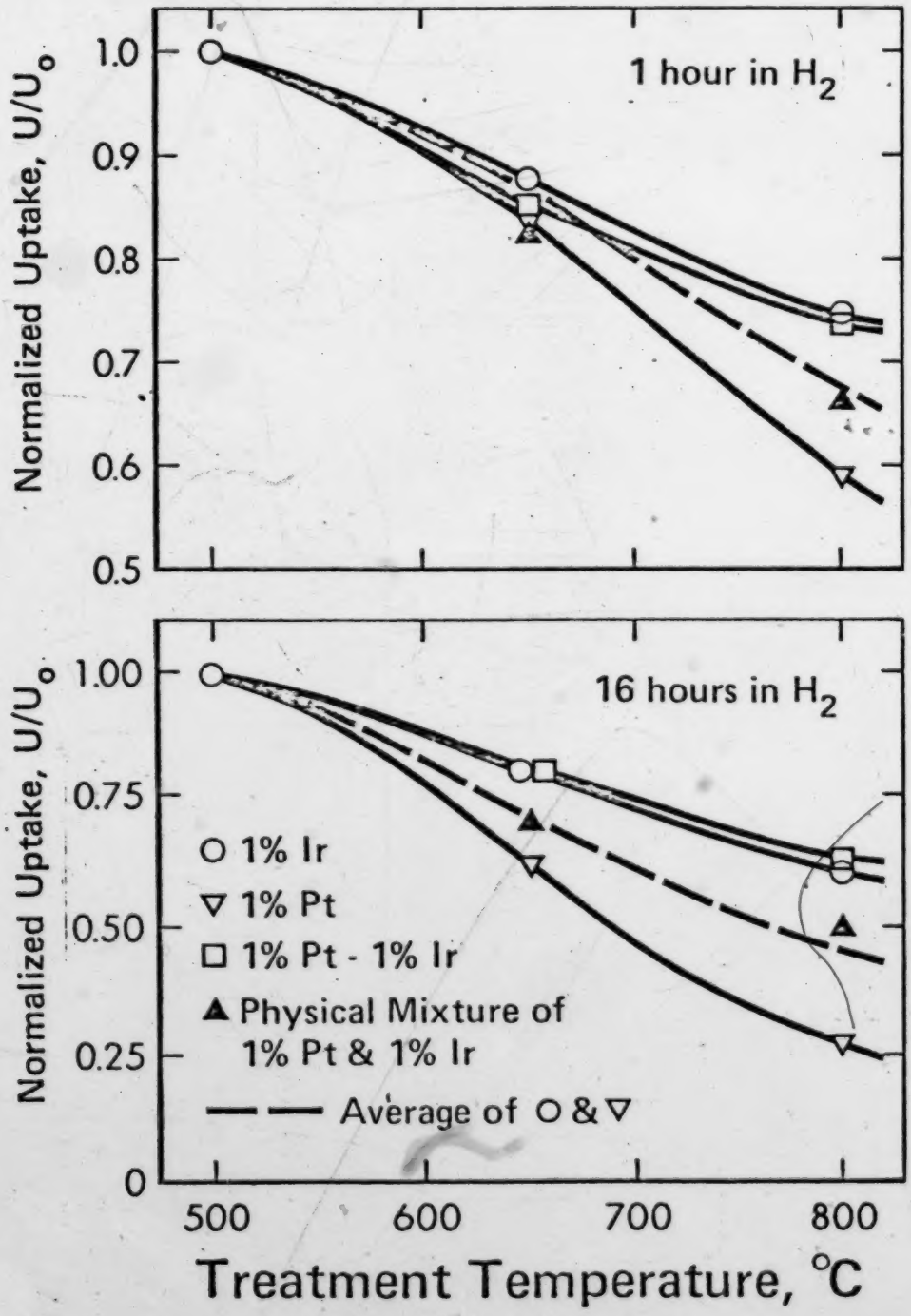

Figure 4.7: Effect of thermal treatment for 1 hour and 16 hours in hydrogen on the normalized uptake for the Platinum and Iridium Catalysts.

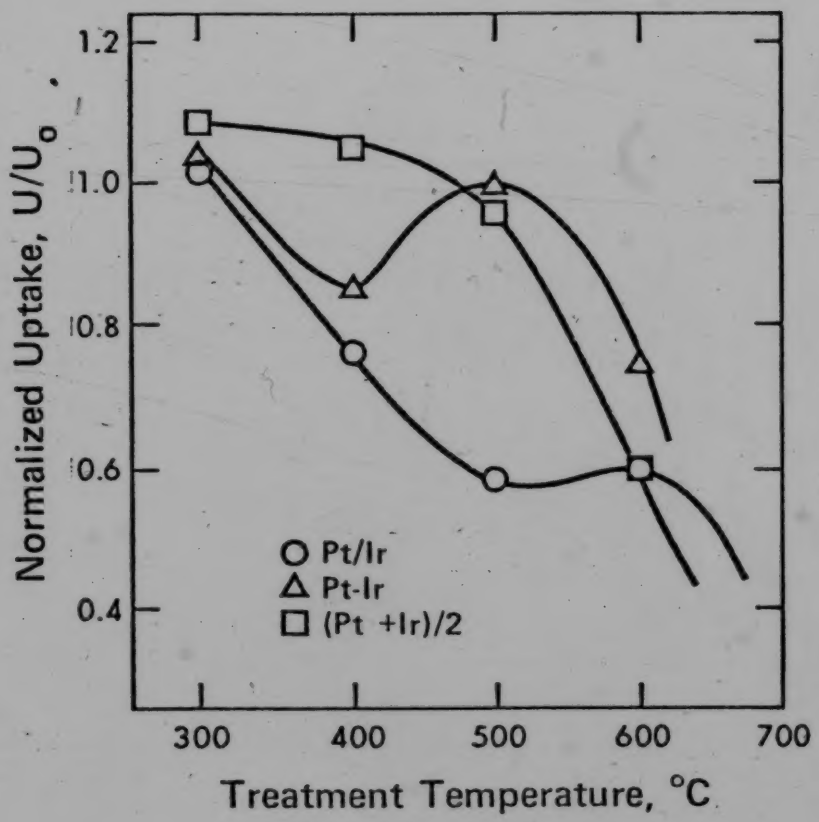

Figure 4.8: Effect of thermal treatment for 1 h in oxygen on the normalized uptake for 1%Pt/1%Ir/Alon and a 50/50 mechanical mixture of 1%Pt/Alon and 1%Ir/Alon.

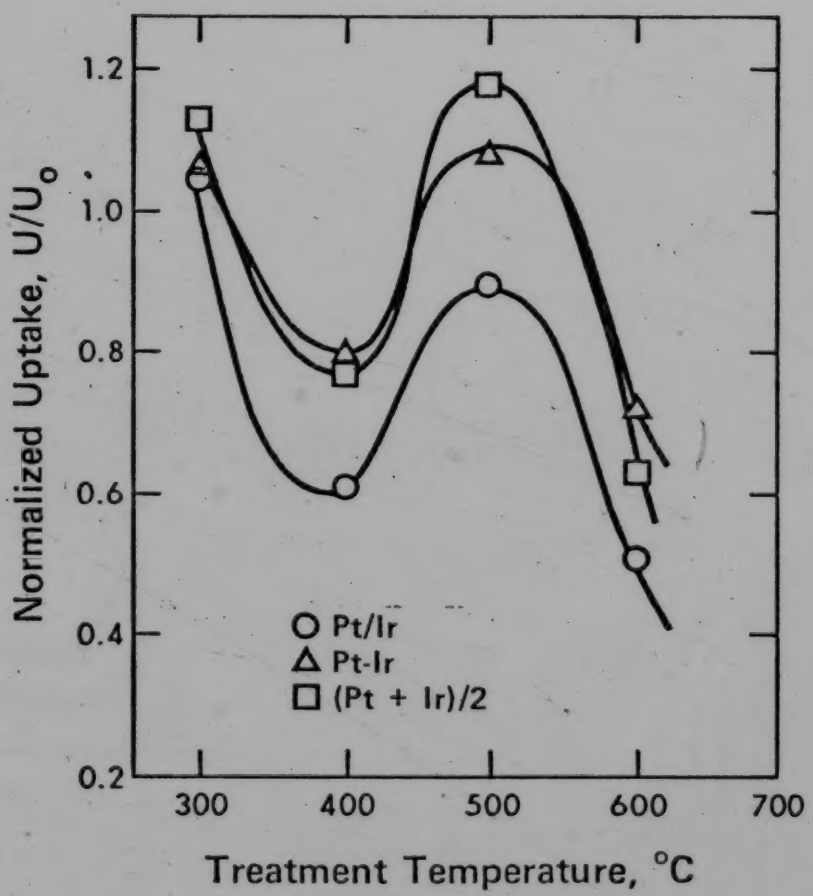

Figure 4.9: Effect of thermal treatment for 16 h in oxygen on the normalized uptake for 1%Pt/1%Ir/Alon and a 50/50 mechanical mixture of 1%Pt/Alon and 1%Ir/Alon.

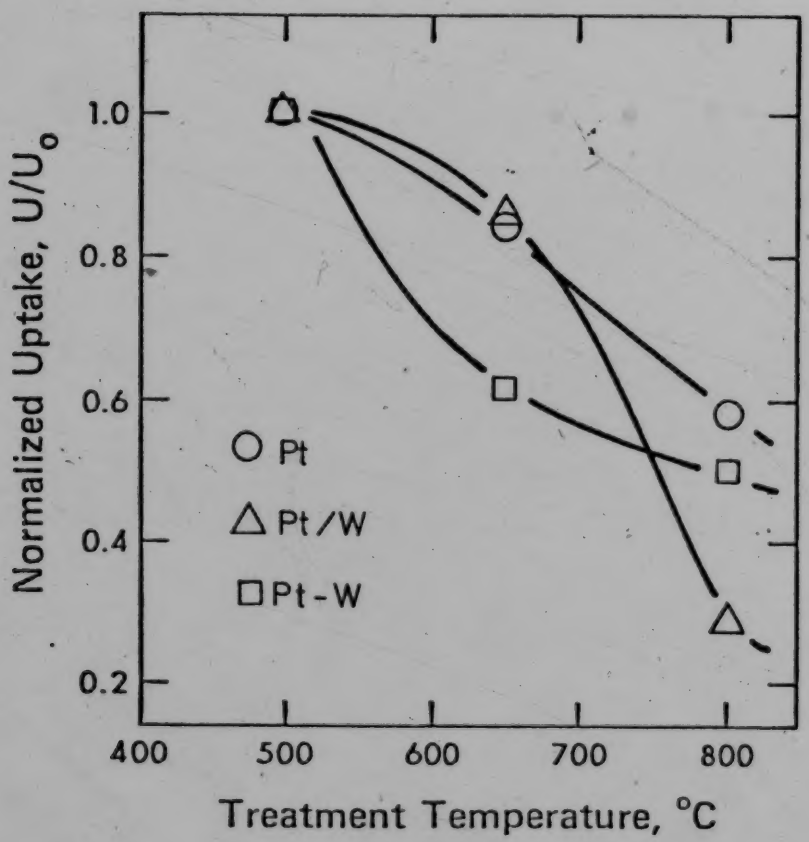

Figure 4.10: Effect of thermal treatment for 1 h in hydrogen on the normalized uptake for 1%Pt/Alon, 1%Pt/1%W/Alon and a 50/50 mechanical mixture of 1%Pt/Alon and 1%W/Alon

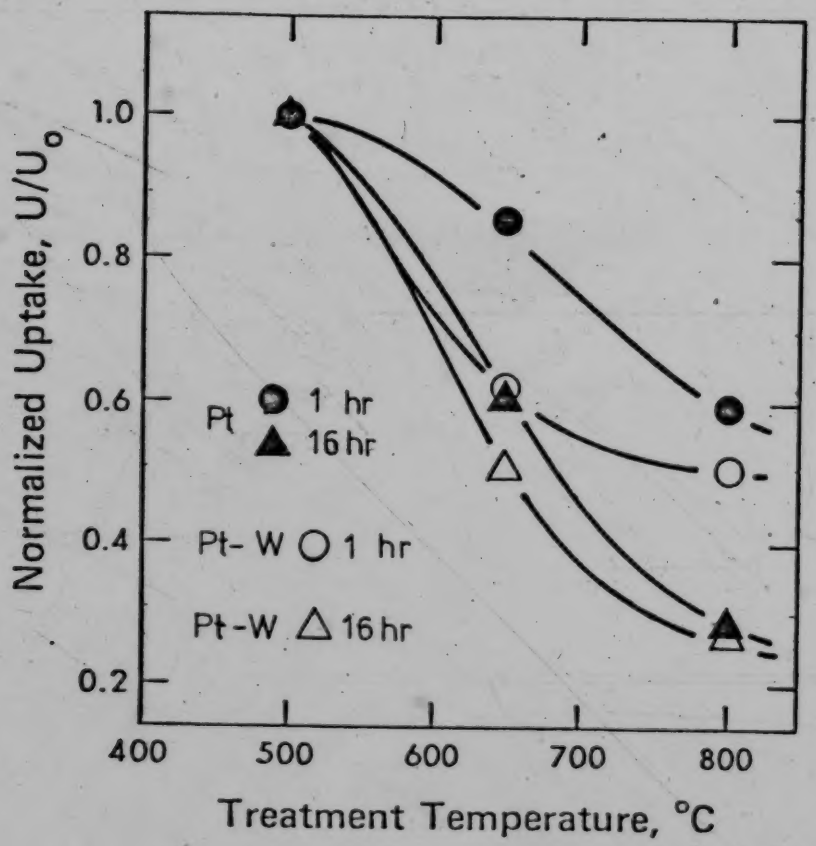

Figure 4.11: Effect of thermal treatment for 1 h and 16 h in hydrogen on the normalized uptake for 1%Pt/Alon and a 50/50 mechanical mixture of 1%Pt/Alon and 1%W/Alon

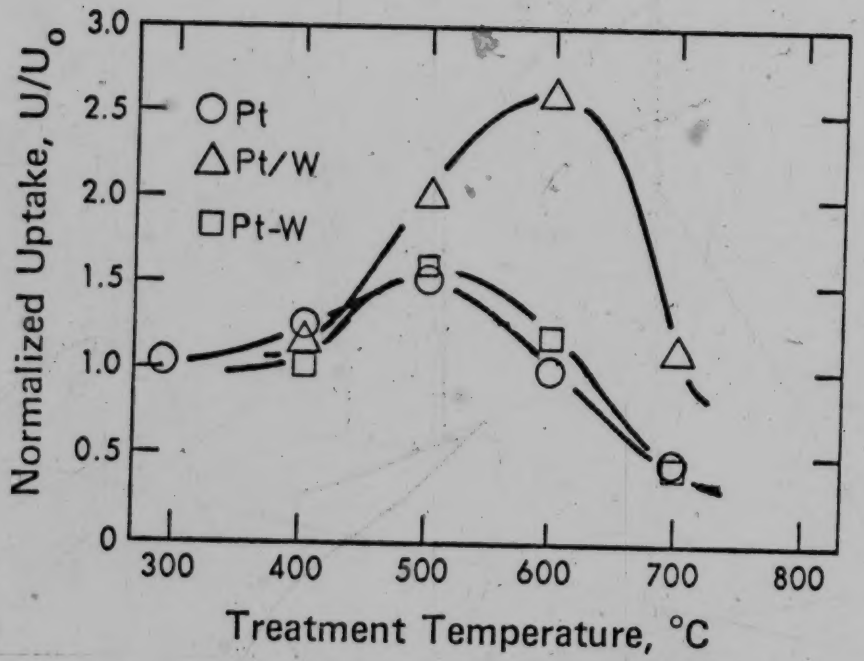

Figure 4.12: Effect of thermal treatment for 1 h in oxygen on the normalized uptake for 1%Pt/Alon, 1%Pt/1%W/Alon and a 50/50 mechanical mixture of 1%Pt/Alon and 1%W/Alon

stability of the monometallic Ir catalyst (see Figure 4.7). It was surprising that the Pt in the bimetallic catalyst seemed to have no effect on the sintering and that the rate of sintering was controlled by the presence of the Ir. These results show that there was a strong interaction between the Pt and the Ir in the bimetallic catalyst. Recently Ramswamy et al. (39) looked at the role of Ir in stabilizing the metal dispersion of Pt on alumina in hydrogen. He found for his catalysts that there were no significant differences between the sintering rates of Pt/Al_2O_3 and $Pt/Ir/Al_2O_3$. This is contrary to the findings of this study and also to the findings of Sinfelt (40) and Kozlov et al. (41).

The thermal stability of the mechanical mixture of the monometallic catalysts followed closely the arithmetic average of the Pt and Ir sintering curves. This indicated that in the mixture, the metals sintered independently of each other as one might expect if there is no long range metal transport or long range metal interactions.

Figures 4.8 and 4.9 show the thermal stabilities of the bimetallic Pt/Ir and the mechanically mixed Pt and Ir catalysts sintered in oxygen. Also included is the arithmetic average curve of the Pt and Ir sintering curves.

Sintering for 1 h in oxygen the bimetallic Pt/Ir catalyst decreased in hydrogen uptake between 300 and 500 °C and then seems to level off between 500 and 600 °C. The Pt-Ir mechanical mixture sintered differently. The curve was different from that for the bimetallic catalyst and that for

the arithmetic average of the Pt and Ir sintering curves. This indicated that within the first hour of sintering there seemed to be some long range interaction between the metals in the mixture. There was certainly an interaction between the Pt and Ir metals on the bimetallic catalyst. After sintering for 16 h in oxygen, the bimetallic Pt/Ir and the Pt-Ir mechanical mixture had the same shape of sintering curve as that for the arithmetic average of the Pt and Ir monometallic catalysts. The closeness of the sintering data for the mechanical mixture with that of the arithmetic average suggests that the metals in the mechanical mixture sintered independently of each other. The same general shape of the bimetallic would lead to the same conclusion that the metals sintered independently. The displacement of the bimetallic curve could be explained by the heavier metal loading (i.e. 2 wt% compared to the 1 wt% for the monometallic catalysts).

The actual composition of the crystallites in the bimetallic Pt/Ir catalyst was not known. The sintering data showed that there was an interaction between the Pt and Ir metals when the catalyst was sintered in hydrogen for 1 and 16 hours and when sintered in oxygen for 1 hour. An interaction between the metals would be expected if the metals were alloyed in the crystallites. The existence of alloyed crystallites or 'bimetallic clusters' has been reported for other metals by Sinfelt (42) and Garten (43). Sintering the bimetallic Pt/Ir catalyst in oxygen for 16 h indicates no interaction between the Pt and Ir and that the metals are segregated on the support surface and sinter independently of

each other. Segregated crystallite formation has been reported for Pt/Re (44). Segregation of Pt and Ir in the bimetallic catalyst could occur for two reasons: First if the metal ions were segregated on the support during impregnation they might have been reduced in clusters of separated metal. Second, the fact that there is an immiscibility gap for the Pt-Ir system would tend to rule out complete miscibility of the two metals in the crystallites. The equilibrium phase diagram for the Pt-Ir system is shown in Figure 4.13 (45) and indicates the formation of two phases, one being essentially Ir and the other essentially Pt.

Recently, Rasser (46) found evidence for the formation of alloyed Pt/Ir crystallites. He reviewed the thermodynamic data for the Pt-Ir system and found that the immiscibility phase diagram is more complicated than previously reported. He found that for an atom fraction, x, for Ir, separation into two phases with compositions of $Pt_{0.95}\ Ir_{0.05}$ and Pt_3Ir is expected for $0.05 \leq x \leq 0.25$. For $0.25 \leq x \leq 0.99$ the phase diagram predicts the formation of two phases, Pt_3Ir and $Pt_{0.01}\ Ir_{0.99}$. Although the phase boundaries of the miscibility gap are dependent on the size of the bimetallic Pt/Ir crystallites (48, 49) it is likely the crystallites formed with two phases each having some Ir with the Pt. (Since the bimetallic catalyst in this study 50/50 Pt/Ir, crystallites of Pt_3Ir and $Pt_{0.01}\ Ir_{0.99}$ should have formed and by the lever rule (48) there should have been twice as much by wt. of the Pt_3Ir phase than the $Pt_{0.01}\ Ir_{0.99}$ phase.) The ways in which Ir could interact with Pt to affect the thermal stability of the Pt

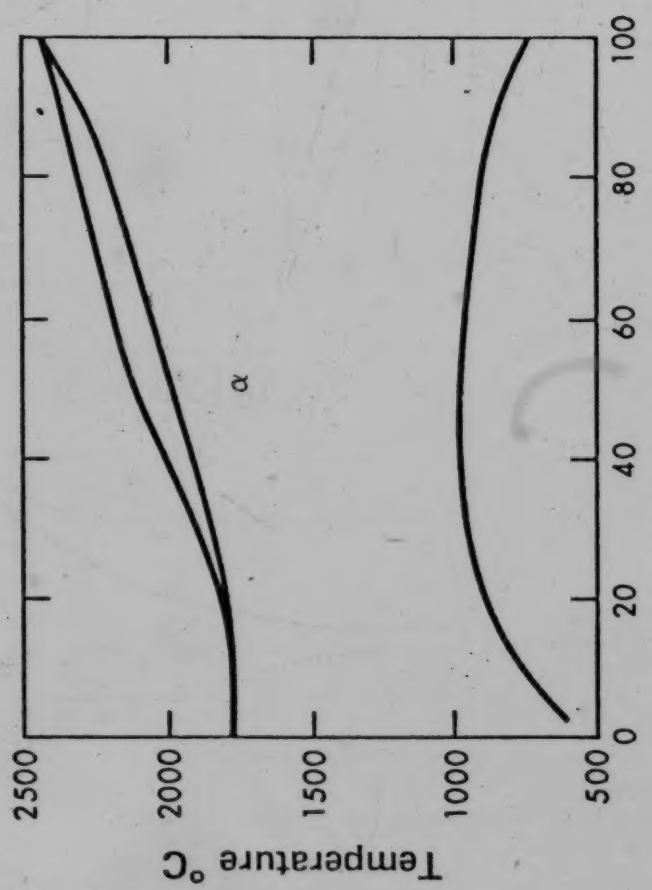

Figure 4.13: The equilibrium phase diagram for Pt-Ir

in the bimetallic catalyst are:

1. The presence of Ir could increase the activation energy required for an atcm to escape from the crystallite surface when sintered in hydrogen;

2. The Ir could alter the formation of the mobile oxide species when sintering in oxygen;

3. The growth of the crystallites should be governed by thermodynamic restrictions imposed on the crystallite composition; therefore, Ir transfer as well as Pt transfer is required. The transfer of Ir could be rate contrclling.

4. Depletion of Pt from the crystallite surface would mean enrichment of the Ir. Since Ir has the higher surface free energy, this condition could also slow rate of sintering.

Rasser notes that for small crystallites the actual composition of the crystallite may not necessarily be the same as that predicted from the equilibrium phase diagram for the bulk metal.

The sintering atmosphere can significantly affect the composition of the bimetallic crystallite (50). This could be a possible reason why there was apparently no interaction between the Pt and Ir when the bimetallic was sintered in oxygen for 16 h. In the preparation of the catalysts the crystallites were formed by the reduction of the metal salt in a hydrogen atmosphere. Sintering in oxygen may have caused a change in the crystallite composition (i.e. separation of the

phases into the individual metals). The changing composition may have been the reason for some interaction in the first hour of sintering in oxygen. After the initial stages of sintering the metals, Ir and Pt, appeared to sinter independently (see the 16 h in oxygen results). The interaction observed for the mechanical mixture after 1 h sinter in oxygen was probably due to vapour phase transport of iridium oxide.

4.6.2 Supported Bimetallic Pt/W Catalysts

The sintering curves for bimetallic 1%Pt/1%W and mechanical mixtures of 1%Pt and 1%W monometallic catalyst are given in Figures 4.10-4.12. It is difficult to make meaningful comparisons of the results with those of the Pt catalyst and the Pt-W mechanical mixture because: one, the initial dispersions are so different; and two, there is the possibility that the tungsten surface complex on the bimetallic Pt/W catalyst is not the same as the the complex on the monometallic W catalyst (51). Note that the average initial dispersion of the Pt-W mechanical mixture was approximately half that for the Pt monometallic catalyst (see Table 3.5). One would expect this for the mechanical mixture if the monometallic W catalyst does not adsorb hydrogen and if there are no interactions of the tungsten catalyst with the chemisorptive properties of the Pt catalyst. Figure 4.10 shows that the addition of W did not stabilize the thermal stability of the Pt as the Ir had done. In fact after 1 h in hydrogen at 800 °C the H/M was less for the bimetallic

catalyst than it was for the monometallic Pt catalyst. The figure also shows that for the Pt-W mechanical mixture there appeared to be some interaction between the Pt and the W catalysts. This can be concluded from the fact that the sintering curve for the Pt-W mechanical mixture should be the same as the monometallic Pt catalyst assuming the W catalyst in the mixture neither adsorbs hydrogen nor affects the chemisorptive properties of the Pt catalyst. No interaction between the Pt and W was found when the mixture was sintered for 16 h in hydrogen (see Figure 4.11).

Figure 4.12 gives the thermal stability curve for the bimetallic Pt/W and the mechanically mixed Pt and W monometallic catalysts sintered in oxygen for 1 h. In this case the sintering of the mechanical mixture was close to the sintering of the Pt monometallic catalyst and indicates no interaction in the sintering of the Pt and W. The bimetallic catalyst shows substantial redispersion between 500 and 700 °C.

Similar results have been observed by Ioffe and co-workers (52). Ioffe prepared two catalysts; 4.2% W/2.9% Pt (cat.1) and 6% W/3% Pt (cat.2) by impregnating silica with solutions of tetrakis-π-methallyltungsten and bis-π-methallylplatinum. After a 600 °C reduction cat.1 had an H/M of 0.3 and cat.2 had an H/M of 0.12. The 1%W/1%Pt/alumina catalyst in this study had a H/M of 0.067. From X-ray diffraction, Ioffe concluded that although the H/M was low the X-ray data did not indicate the formation of large

crystallites. This is in agreement with our X-ray results. Ioffe concluded from his studies the Pt was actually highly dispersed. He mentions nothing as to the actual state of the W on the support but does give two explanations for the observed influence of the W on the hydrogen uptake of Pt: one, the tungsten could modify the surface of the Pt crystallites thus modifying the adsorption properties of the Pt; and two, an interaction could occur between clusters of Pt atoms and low valent ions of W bound to the support thus affecting the adsorption properties of the Pt.

Preparation of Pt/W supported bimetallic catalysts have been reported by others (53); however no mention is made as whether the W had been reduced to the metallic state or not.

The role of W (likely as a surface complex) in the sintering mechanism is nct clear. It is probable that the tungsten plays a bigger role in altering the adsorption properties of Pt than in affecting how it sinters. This is also indicated from the observation that the second hydrogen adsorption uptake was usually greater than the first uptake. This is opposite to the results found for the platinum and iridium catalysts (see Table 3.6).

It is likely that the large hydrogen uptakes found for the bimetallic Pt/W catalyst sintered in oxygen were not due to substantial redispersion but rather due to decreased interference of the tungsten complex with the adsorption properties of the Pt. How the oxygen environment affects the tungsten surface complex and the adsorptive properties of the

Pt is not known.

4.7 Summary of the Sintering Behaviour of the Catalysts

A qualitative comparison of monometallic sintering behaviour of the 1%Pt, 1%Ir and 1%W supported on Alon and bimetallic 1%Pt/1%Ir, 1%Pt/1%W supported on Alon was made.

The sintering results for the Pt and Ir monometallic catalysts were similar to results published in the literature. The Ir catalyst had greater thermal stability in hydrogen than the Pt catalyst. The Pt catalyst had better thermal stability and greater redispersion in oxygen than did the Ir catalyst. The W monometallic catalyst did not adsorb hydrogen. The W on the Alon support could not be reduced to the metal.

The bimetallic Pt/Ir catalyst had the same thermal stability as the Ir catalyst when sintered in hydrogen. This indicated an interaction between the Pt and the Ir which affected the sintering behaviour of the bimetallic catalyst. The mechanical mixture of 50% Pt monometallic and 50% Ir monometallic catalyst showed that the metals in the mixture sintered independently in the hydrogen atmosphere. In oxygen the Pt/Ir bimetallic catalyst was less thermally stable than in hydrogen. There was interaction between the Pt and Ir on the bimetallic catalyst in the first hour of sintering in oxygen. There appeared to be no interaction between the metals when the catalyst was sintered for 16 h in oxygen. The Pt-Ir mechanical mixture showed some interaction between the Pt and Ir when sintered in oxygen.

A meaningful comparison of the sintering behaviour of the Pt/W bimetallic catalyst with the monometallic Pt catalyst was difficult due to the large differences in the initial dispersions of the two catalysts.

The presence of W in the bimetallic catalyst did not appear to increase the stability of the Pt. Comparison of the results of the bimetallic Pt/W catalyst with the results for the Pt-W mechanical mixture indicated that an interaction between the Pt and W on the bimetallic catalyst affected the rate of sintering of the catalyst. It was felt that the presence of the W as a surface complex had a greater effect on the chemisorptive properties of the Pt than on the rate of sintering.

CHAPTER 5

CONCLUSIONS

1. The thermal stability sequence for catalysts sintered in hydrogen is: 1%Pt/Alon < 1%Ir/Alon ≅ 1%Pt/1%Ir/Alon.

2. 1%Pt/Alon showed a maximum redispersion in oxygen at 500 °C.

3. The thermal stability of 1%Pt/Alon is greater than that for 1%Ir/Alon for sintering in oxygen.

4. Interactions between Pt and Ir on the bimetallic catalyst were found to influence the sintering rate of the metals in hydrogen and for 1 h sintering in oxygen. No interaction between the metals was found when the bimetallic catalyst was sintered in oxygen for 16 h.

5. X-ray diffraction data showed the formation of large metal crystallites when the monometallic Pt and Ir catalysts and the bimetallic Pt/Ir catalyst were sintered in oxygen at >600 °C. No large crystallite formation occurred when the catalysts were sintered in hydrogen at 800 °C for 16 h although the hydrogen uptakes were low.

6. Special sintering experiments were inconclusive in proving the existence of non-hydrogen adsorbing Pt and Ir surface complexes on Alon.

7. The W monometallic catalyst prepared by impregnation of Alon with ammonium metatungstate did not adsorb hydrogen. This was due to the W reacting with the alumina support.

8. A maximum relative uptake of 2.56 after sintering in oxygen occurred at 600 °C for the Pt/W bimetallic catalyst.

9. The presence of tungsten in the 1%Pt/1%W bimetallic catalyst did nct increase the thermal stability of the Pt.

10. An interaction between the Pt and W on the bimetallic Pt/W catalyst was observed in both oxygen and hydrogen sintering atmospheres. It is believed that the tungsten affected the chemisorptive properties of the Pt.

11. BET measurements showed that no appreciable surface area changes of the Alon support occured during the sintering experiments. X-ray diffraction studies showed that there was no appreciable increase in the support crystallinity.

12. The results suggest an atomic migration model for crystallite growth. In oxygen the migrating species are oxides. Migration of the oxide species occured by transport across the support surface. There is also some evidence, at least for Ir, of vapour phase metal transport.

CHAPTER 6

RECOMMENDATIONS

Based on the findings of this study further investigation is required in the following areas:

1. Unambiguous results are required to establish whether or not Pt forms a non-hydrogen adsorbing complex with Alon during treatment in hydrogen.

2. Experiments should be carried out to clarify the reason for the observed differences in the first and second hydrogen uptake measurements.

3. A study should be made on the effect of varying metal composition in the bimetallic catalysts especially for the Pt/Ir catalyst with Pt concentrations > 75%.

4. The effect of metallic tungsten on the thermal stability of Pt should be studied on a support that does not react with the tungsten.

REFERENCES

1. Ruckenstein, E., and Pulvermacher, B., AIChE J. 19, 356 (1973).

2. Flynn, P.C., and Wanke, S.E., J. Catal. 34, 390 (1974).

3. Wanke, S.E., and Flynn, P.C., Catal. Rev. 12, 93, (1975).

4. Gruber, H.L., J. Phys. Chem. 66, 48 (1962).

5. Mueller, J., Rev. Pure Appl. Chem. 19, 151 (1969).

6. Schlosser, E.G., Chem. Ing. Technik. 39, 409 (1967).

7. Freel, J., J. Catal. 25, 139 (1972).

8. Flynn, P.C., Ph.D. Thesis, University of Alberta, Edmonton, 1974.

9. Klug, H.P., and Alexander, L.E., "X-ray Diffraction Procedures", chap. 9, Wiley, New York, 1954.

10. Halliday, D., and Resnick, R., "Physics, Parts I and II", p. 1142, Wiley, New York, 1967.

11. Wilson, G.R., and Hall, W.K., J. Catal. 17, 190 (1970).

12. Flynn, P.C., and Wanke, S.E., J. Catal. 34, 400 (1974).

13. Miller, I., and Freud, J.E., "Probability and Statistics for Engineers", p. 119, Prentice Hall, Englewood Cliffs, N.J., 1965.

14. Fiedorow, R.M.J., and Wanke, S.E., J. Catal. 43, 34 (1976)

15. Fiedorow, R.M.J., Chahar, B.S., Wanke, S.E., J. Catal. 51, 193 (1978).

16. McKee, D.W., and Norton, F.J., J. Phys. Chem. 68, 481 (1964).

17. Gray, T.J., Masse, N.G., Oswin, H.G., "Actes 2ieme Congr. Int. Catal., Vol. 2", p. 1697, Technip. Paris (1961).

18. Chem. Abstr. 84, 76689m (Ger. Offen. 2,443,976).

19. Maatman, R.W., and Prater, C.D., Ind. Eng. Chem. 49, 253 (1957).

20. Hunt, C.E., J. Catal. 23, 93 (1971).

21. Flynn, P.C., and Wanke, S.E., Can. J. Chem. Eng. 53, 636 (1975).

22. Gruber, H.L., Anal. Chem. 34, 1828 (1962).

23. Biloen, P., and Pott, G.T., J. Catal. 30, 169 (1973).

24. Massoth, F.E., J. Catal. 30, 204 (1973).

25. Sondag, P., Kim, D.Q., Marion, F., Compt. Rendu. 259, 4704 (1964).

26. Sprys, J.W., and Mencik, Z., J. Catal. 40, 290 (1975).

27. Dautzenberg, F.M., and Wolters, H.B.M., J. Catal. 51, 26 (1978).

28. Ruckenstein, E., and Pulvermacher, B., J. Catal. 29, 224 (1973).

29. Wynblatt, P., and Gjostein, N.A., Scr. Met. 7, 969 (1973).

30. Wynblatt, P., and Gjostein, N.A., Acta Met. 24, 1165 (1976).

31. Flynn, P.C., and Wanke, S.E., J. Catal. 37, 432 (1975).

32. Chahar, B.S., M.Sc. Thesis, University of Alberta, Edmonton, 1976.

33. Anderson, J.R., "Structure of Metallic Catalysts", p. 446, Academic Press, San Francisco, 1975.

34. Wynblatt, P., and Ahu, T.-M., "Sintering in Catalysis", (G.C. Kuczynski, Ed.), p. 83, Plenum, New York, 1975.

35. Chaston, J.C. Plat. Met. Rev. 9, 51 (1965).

36. McVicker, G.B., Garten, R.L., Baker, R.T.K., "5th Canadian Synposium on Catalysis, Preprints", p. 346

37. Harriot, P., J. Catal. 14, 43 (1969).

38. Anderson, J.R., "Structure of Metallic Catalysts", p. 176, Academic Press, San Francisco, 1975.

39. Ramaswamy, A.V., Ratnasamy, P., Sivasanker, S., "Proc. 6th Int. Cong. Catal., Vol. II", p. 855, London (1976).

40. Chem. Abstr. 82, 46223w (1975) (U.S. Patent 3,835,034).
Chem. Abstr. 82, 61743j (1975) (U.S. Patent 3,839,194).

41. Kozlov, N.S., Mostovaya, L.Ya., Zhizhenko, G.A., Neftekhimiya, 14, 591 (1974).

42. Sinfelt, J., Acc. Chem. Res. 10, 15 (1977).

43. Garten, R.L., J. Catal. 43, 18 (1976).

44. Peri, J.B., J. Catal. 52, 144 (1978).

45. Darling, A.S., Plat. Met. Rev. 4, 18 (1960).

46. Rasser, J.C., "Platinum-iridium reforming catalysts", chap. 3, Delft University Press, Delft, Netherlands (1974)

47. Darken, L.S., and Gurry, R.W., "Physical Chemistry of Metals", p. 316, McGraw-Hill, Toronto, 1953.

48. Ollis, D., J. Catal. 23, 131 (1971).

49. Hoffman, D.W., J. Catal. 27, 374 (1972).

50. Anderson, J.R., "Structure of Metallic Catalysts", p. 157, Academic Press, San Francisco, 1975.

51. Kohn, H.W., and Boudart, M., Science 145, 149 (1964).

52. Ioffe, M.S., Kuznetsov, B.N., Ryndin, Yu.A., Yermakov, Yu. I., "Proc. 6th Int. Congr. Catal., Vol. I", p. 131, London (1976).

53. Aboul-Gheit, A.K., Cosyns, J., Revista Del Instituto Mexicano Del Petroleo VII, 61 (1975).

54. "Handbook of Chemistry and Physics", 48th ed., p. F-1, Chemical Rubber Co., Cleveland, 1970.

55. Rollinson, C.L., "Comprehensive Inorganic Chemistry, vol. 3", (J.C. Bailer , Ed.), sect. III p. 742, Pergamon Press, Oxford, 1973.

56. Zachariasen, W.H., "Theory of X-ray Diffraction in Crystals", p. 99, Dover Publications, New York, 1967.

APPENDIX A

A-1.1 Introduction

In this appendix the method used to calibrate the sample loops on the gas sample valve is described. Also a sample dispersion calculation and a sample BET surface area measurement calculation is presented.

A-1.2 Calibration of Sample Loop

The metal dispersion (or H/M) of the catalysts used in this study was found by hydrogen chemisorption. The amount of hydrogen chemisorbed was measured using the dynamic flow adsorption method. This method used two sample loops(designated loop1 and loop2) on a gas sample valve to inject hydrogen into a nitrogen carrier stream which purged through the catalyst bed. In order to calculate the dispersion the number of moles of hydrogen contained in the sample loops had to be determined. The method used here was to inject known volumes of hydrogen using a gas syringe and then compare the T.C. cell response to that when hydrogen was injected by the gas sample valve.

The experimental equipment was made ready as if an actual catalyst sample was being run except that no catalyst was placed in the sample holder. A syringe injection port was positioned in line immediately down stream from the gas sample valve. The placement of the port right after the valve was necessary so as to give the same broadening of the peak from

the syringe injected hydrogen pulse as one normally observes using the sample valve.

A 1 cc gas-tight syringe (Hamilton Co. Inc. Whittier Calf., Gastight #1001) was used to inject hydrogen. The syringe was calibrated using water. The syringe was weighed empty and with volumes of 0.2, 0.4 and 0.5 cc of water. The average water temperature was 21.7 °C and the density was taken as 0.997837 g/cc (54). The calibrated volumes are given in Table A-1.1.

After the syringe was calibrated samples of hydrogen were drawn from a gas sampling bulb which had been flushed and filled with hydrogen. The side-arm of the bulb was fitted with a septum for syringe sampling. Volumes of 0.2, 0.4 and 0.5 cc of hydrogen were injected several times. The peaks and their areas were recorded on the H.P. 3380A integrator. The results are shown in Table A-1.2. The injection port was removed from the line and pulses of hydrogen were injected using the gas sample valve. The areas of these peaks are given in Table A-1.3.

The moles of hydrogen injected by the syringe were found by adjusting the actual volumes (from Table A-1.1) to STP using the ambient temperature and pressure recorded in Table A-1.2. As a matter of preference the volume of hydrogen at STP was used rather than converting it to a mole quantity. The conversion can be readily done by assuming ideal gas behaviour so that 1 mole of gas = 22414 cc. The actual

Table A-1.1

Syringe Calibration

Syringe Vol. in mls.		Wt. of Water in gms.	Actual Vol. in mls.*
0.5		0.5015	
		0.5008	
		0.4999	
		0.5032	
	AVG.=	0.5014	0.5024
0.4		0.4026	
		0.3981	
		0.3972	
		0.4006	
	AVG.=	0.3996	0.4005
0.2		0.1976	
		0.1986	
		0.2011	
		0.1993	
	AVG.=	0.1992	0.1996

* The temperature of the water was 21.7°C for which the density is 0.997837 grams/mls.

Table A-1.2

Calibration of Peak Areas

Syringe Vol. in mls. *	Area in 'counts' **
0.5	2626452
	2619957
	2626431
0.4	2113052
	2098975
	2117670
	2121835
	2117927
0.2	1043539
	1067950
	1069812
	1079238
	1078462
	1079559

* The temperature and pressure of the hydrogen in the syringe was taken as 298.15 K and 695.7 mmHg.

** The T.C. bridge current was 150 mA and the power supply sensitivity was 2.

Table A-1.3

Sample Loop Size

	Loop 1 Area in 'counts'		Loop 2 Area in 'counts'
	2194792		2147786
	2194768		2149634
	2195873		2148378
	2197263		2150950
	2219516		2156805
	2217845		2169699
	2162043		2126329
	2173328		2130646
	2153590		2130416
	2178224		2161394
	2210431		
AVG.=	2190698	AVG.=	2147204

volumes at STP injected by the syringe and each of the areas in Table A-1.2 were fitted by linear least squares to the equation:

$$\text{VOLUME OF } H_2 \text{ (at STP)} = b \times \text{AREA} \qquad [A-1]$$

were b is the slope. The slope was found to be 1.5926×10^{-7} cc/count.

The average sample loop areas from Table A-1.3 were used in equation [A-1] to calculate the volume of hydrogen in the loops. These results are given in Table A-1.4. In order to use equation [A-1] to calculate the volume of hydrogen in the sample loops the assumption was made that molar response of the T.C. cell was the same for the hydrogen injected by the syringe as it was for the hydrogen injected by the gas sample valve.

The volume of the two sample loops were not exactly the same. Loop1 was 1.96% larger than loop2. To facilitate the calculation of the dispersion the two sample loop volumes were averaged. The volume of one pulse of hydrogen from the gas sample valve was taken as 0.345 cc of hydrogen at STP.

It should be noted here that the moles of hydrogen in the sample loops is dependent on the hydrogen temperature and pressure in the loops. In order to calibrate the loops it was assumed that the temperature and pressure in the loops were always constant. The assumption for the pressure was probably good. The pressure in the loops is dependent on the

Table A-1.4

Sample Loop Calibration

Equation [A-1]

VOLUME OF H_2 (at STP) = 1.5926 X 10^{-7} X AREA [A-1]

	Avg. Area	Vol. of (at STP) (in cc);
Loop 1	2190698	0.3490
Loop 2	2147204	0.3420
		Avg. = 0.3455

Avg. loop volume Volume at STP = 0.345 cc

hydrogen flow rate and the upstream hydrogen pressure. Both these parameters were held constant. The assumption for the temperature was not as good. The temperature of the hydrogen in the sample loop was the same as the ambient temperature. However since the room temperature was controlled at 298.15 +/- 2 K the slight variation in temperature was considered negligible.

A-2.1 Dispersion Calculation

To find the hydrogen chemisorbed by the catalysts, pulses of hydrogen were injected into the nitrogen carrier stream via the gas sample valve at ~3.5 minute intervals. Hydrogen pulses were injected until the eluted peaks, as recorded by the electronic integrator, were the same size (i.e. the area of successive peaks from the same loop were generally within 1% of each other). The fractionally adsorbed peaks were calculated by dividing the difference in area between the full and fractional peak by the full peak area. A linear relationship was assumed between the amount of hydrogen passing through the T.C. cell and the peak area. Because of the 1.96% difference in sample loop size, the pulses adsorbed from loop1 were calculated seperately from those of loop2. Summing the pulse from loop1 and loop2 gave the total number of pulses adsorbed. The volume of chemisorbed hydrogen was found by taking the product of the total pulses and the average sample loop volume (i.e. 0.345 cc). The H/M was determined by calculating:

1. the number of hydrogen atoms adsorbed;

2. the toal number of metal atoms in the catalyst.

The number of hydrogen atoms adsorbed is just twice the volume of hydrogen gas adsorbed times the ratio of Avogadro's number to 22414 cc/mole (assuming ideal gas behaviour). The total number of metal atoms is obtained by multiplying the weight of the metal on the catalyst by the ratio of Avogadro's number to the atomic weight of the metal. The total number of metal atoms in the bimetallic catalysts is just the sum of the metal atom for the two metals.

The relative hydrogen uptake was found by dividing the average H/M for the sintered sample by the average H/M for the unsintered sample.

The calculations were done on Amdahl 470v/6 computing system. The programs used for the calculations and the results of the sintering experiments are given in Appendix B.

A-2.2 Sample Calculation

The equation used for calculating H/M is:

$$H/M = \frac{N * V * F * No}{(W/100)*(M1/MW1+M2/MW2)*No} \qquad [3.1]$$

where:

N=the no. of pulses adsorbed (calculated from the peak areas)
V=the average volume of H_2 in the sample loops=0.345 cc.
F=((1/22414)*(2)) mole of H per cc.
Nc=Avogadro's number
W=the weight of the catalyst sample in grams (a)
M1=the wt.% cf metal 1 on the catalyst

M2=the wt.% of metal 2 on the catalyst
MW1=the atomic weight of metal 1
MW2=the atomic weight of metal 2

(a) W=W/2 for the mechanically mixed catalysts

As an illustration the results from run #71 were used in the following calculation. The sample was a 1%Pt/1%Ir bimetallic catalyst. The weight of the sample used was 1.3890 grams. The areas of the peaks and the fraction of pulses they represent are given in Table A-2.1.

Table A-2.1

Calculation of the Total Pulses Adsorbed
for Run# 71 from Exp.# 37

Area of Peak Loop1	Area of Peak Loop2	Adsorbed Pulses * Loop1	Loop2
122116	888806	0.884	0.180
1021831	1068082	0.033	0.015
1051664	1084496	0.005	
1056420			
		0.922	0.195

Total pulses adsorbed = 1.117

* Adsorbed pulse = $\frac{\text{(full peak area - fractional peak area)}}{\text{(full peak area)}}$

Substituting into equation A-2 where:

N=1.117

V=0.345

F=8.922X10^{-5} moles H per cc.

W=1.3890 gm.

%M1=%M2=1

M1=195.09

M2=192.2

Therefore: H/M = 0.240

The H/M for the set of experiments #68-#71 were as follows:

Table A-2.2

H/M Values for Exp.# 37

Run#	Treatment	H/M
68	unsintered	0.435
69	unsintered	0.433
70	sintered	0.267
71	sintered	0.240

Relative Uptake = (0.267+0.240)/2/(0.435+0.433)/2

= 0.584

A-3.1 Surface Area Determinations

The surface area measurements were done by Mr. Z. Leung.

The support surface area measurements were carried out on a constant volume BET apparatus. The dead volume determinations were done using helium . At least four dead volume determinations were done for each sample and an average of all these values was used. The adsorption procedure consisted of the following steps: one, introducing adsorbate (nitrogen) to a desired pressure into the gas holder which is isolated from the evacuated catalyst holder; two, expanding the adsorbate into the catalyst holder; three, waiting for the pressure to reach a steady state value; four, isolating the sample holder from the gas holder; five, introducing adsorbate to a desired pressure into the gas holder; six, repeating steps two to five at least four times. The amount of nitrogen adsorbed at the various pressures is given by:

$$U_i = \frac{1}{R\,T_g}\left(V_g \sum_{j=1}^{i}(P_j - P_{jj-1}) - P_{ii}(V_g + \bar{V}_d)\right) \qquad [A\text{-}2]$$

where:

Ui=moles of nitrogen adsorbed per gram of catalyst

Vg=volume of the gas holder

$\bar{V}$d=average dead volume

Tg=temperature of gas holder

Pi=pressure in the gas holder after the ith adsorbate

introduction before opening the valve to the catalyst holder

Pii=pressure (steady-state value) in gas holder and catalyst holder after opening the valve to the catalyst for the ith measurement (Pii=0, i=0)

R=gas constant

A plot of $Pii/[Ui(Po-Pii)]$ versus Pii/Po leads to a straight line with a slope a and an intercept b. Po is the saturation pressure of the adsorbate (nitrogen) at the temperature of adsorption. This value was measured with a Wallace-Tiernan pressure gauge. The slope and the intercepts were found by fitting the data points in the range $0.05 \leq P/Po \leq 0.35$ to a straight line using a least squares method. The nitrogen monolayer coverage uptake is given by:

$$Um = 1/(a+b) \qquad [A-3]$$

Once Um is known, the support surface are is calculated using the following equation:

$$A = UmNoAo \qquad [A-4]$$

where A is the support surface area, No is Avogadro's number and Ao is the area covered per nitrogen molecule which is taken to be equal to 15.8×10^{-20} m^2. A sample calculation is shown below.

3.2 Sample Calculation of BET Surace Area Measurement

This sample calculation is for a fresh sample of the 1%Pt/1%Ir bimetallic catalyst.

Outgas Temp.: 250 °C Outgas Time: 16 hours

Sample Weight: 1.0035 g Po = 721.0 Torr
= 13.946 lbs/sq. in.
T = 23.0°C = 296.15 K

a) Dead Volume Vd Determination:

Volume of gas holder, Vg = 145.92 ml

P1(psia)	P2(psia)	Vd(ml) = Vg(P1-P2)/P2
4.507	3.283	54.4033
3,297	2.400	54.5376
3.999	2.915	54.2632
2.927	2.130	54.6001
4.307	3.137	54.4234
3.112	2.269	54.2135

Average Vol., Vd= 54.406

b) Adsorption Data:

i	Pi(psia)	Pii(psia)	Pii/Po
1	2.222	0.285	0.0204
2	2.264	1.326	0.0951
3	2.302	1.882	0.1350
4	2.403	2.183	0.1565
5	2.501	2.361	0.1693
6	2.702	2.556	0.1833
7	2.904	2.751	0.1973
8	3.206	3.016	0.2163
9	3.502	3.298	0.2365
10	3.900	3.648	0.2616
11	4.300	4.026	0.2887
12	4.702	4.414	0.3165
13	4.852	4.661	0.3342
14	5.005	4.854	0.3481
15	12.021	8.840	0.6339
16	20.002	12.290	0.8813

c) Computation of Um and Surface Area:

i	Pii/Po	UiX10^4	Pii/(Ui(Po-Pii))
1	0.0204	7.456	27.979
2	0.0951	9.696	108.368
3	0.1350	10.562	147.701
4	0.1565	11.001	168.697
5	0.1693	11.301	180.339
6	0.1833	11.599	193.466
7	0.1973	11.926	206.044
8	0.2163	12.298	224.381
9	0.2365	12.700	243.875
10	0.2616	13.195	268.465
11	0.2887	13.737	295.439
12	0.3165	14.321	323.356
13	0.3342	14.724	340.943
14	0.3481	15.046	354.840
15	0.6339	21.948	788.837
16	0.8813	48.120	1542.601

Pii/(Ui(Po-Pii)) versus Pii/Po was fitted to a straight line using a linear least squares routine for the points i=2 to i=14. The slope was found to be 970.906 g/mole and the intercept was 15.625 g/mole.

$Um = 1/(970.906 + (15.625)) = 1.014 \times 10^{-3}$ moles/gram

$Area = 1.014 \times 10^{-3}$ (moles) $\times 6.023 \times 10^{23} \times 15.8 \times 10^{-20}$ (m^2/molecule)

$= 96.4\ m^2/g$

APPENDIX B

Table B-1 lists the hydrogen chemisorption data. It includes sample weight, treatment conditions, number of hydrogen pulses adsorbed and the hydrogen to metal ratio (H/M). Note that under the heading CAT an AY indicates that the sample was a co-impregnated bimetallic catalyst while an MX was used to denote the mechanical mixtures.

Table B-2 lists the hydrogen chemisorption runs that were omitted from Table B-1 and gives the reasons why the runs were omitted.

Table B-3 lists the computer programs used to calculate the H/M given in Table B-1. The first program is for the monometallic catalysts and the second program is for the co-impregnated bimetallic and mechanically mixed catalysts.

Table B-1

The Hydrogen Chemisorption Data

EXP	CAT	RUN #	PRETREATMENT ATM	TEMP (°C)	TIME (h)	SAMPLE SIZE (gm)	NUMBER OF PULSES ADSORBED	H/M
1	IRIDIUM	26	UNSINTERED			1.7358	1.218	0.416
	IRIDIUM	27	UNSINTERED			1.7358	1.210	0.413
	IRIDIUM	28	OXY	300	1	1.7358	1.411	0.481
	IRIDIUM	29	OXY	300	1	1.7358	1.449	0.494
						RELATIVE UPTAKE =		1.178
2	IRIDIUM	120	UNSINTERED			1.6000	1.154	0.427
	IRIDIUM	121	UNSINTERED			1.6000	1.163	0.431
	IRIDIUM	122	OXY	400	1	1.6000	0.965	0.357
	IRIDIUM	123	OXY	400	1	1.6000	0.949	0.351
						RELATIVE UPTAKE =		0.827
3	IRIDIUM	36	UNSINTERED			1.7089	1.206	0.418
	IRIDIUM	37	OXY	500	1	1.7089	0.488	0.169
	IRIDIUM	38	OXY	500	1	1.7089	0.462	0.160
						RELATIVE UPTAKE =		0.394
4	IRIDIUM	255	UNSINTERED			1.6364	1.306	0.473
	IRIDIUM	256	OXY	600	1	1.6364	0.267	0.097
	IRIDIUM	256	OXY	600	1	1.6364	0.267	0.097
						RELATIVE UPTAKE =		0.205

EXP	CAT	RUN #	PRETREATMENT ATM	TEMP (°C)	TIME (h)	SAMPLE SIZE (gm)	NUMBER OF PULSES ADSORBED	H/M
5	IRIDIUM	278	UNSINTERED			1.7020	1.322	0.460
	IRIDIUM	279	UNSINTERED			1.7020	1.261	0.439
	IRIDIUM	280	OXY	300	16	1.7020	1.599	0.556
	IRIDIUM	281	OXY	300	16	1.7020	1.540	0.536
							RELATIVE UPTAKE =	1.216
6	IRIDIUM	20	UNSINTERED			1.8836	1.299	0.409
	IRIDIUM	21	UNSINTERED			1.8836	1.293	0.407
	IRIDIUM	24	OXY	400	16	1.8836	0.439	0.138
	IRIDIUM	25	OXY	400	16	1.8836	0.402	0.127
							RELATIVE UPTAKE =	0.325
7	IRIDIUM	15	UNSINTERED			1.9195	1.455	0.449
	IRIDIUM	17	OXY	500	16	1.9195	0.343	0.106
	IRIDIUM	18	OXY	500	16	1.9195	0.324	0.100
							RELATIVE UPTAKE =	0.230
8	IRIDIUM	39	UNSINTERED			1.7428	1.181	0.401
	IRIDIUM	40	OXY	500	16	1.7428	0.305	0.104
	IRIDIUM	41	OXY	500	16	1.7428	0.304	0.104
							RELATIVE UPTAKE =	0.258

EXP	CAT	RUN #	PRETREATMENT ATM	TEMP (°C)	TIME (h)	SAMPLE SIZE (gm)	NUMBER OF PULSES ADSORBED	H/M
9	IRIDIUM	251	UNSINTERED			1.6612	1.247	0.445
	IRIDIUM	252	UNSINTERED			1.6612	1.241	0.443
	IRIDIUM	253	OXY	600	16	1.6612	0.282	0.101
	IRIDIUM	254	OXY	600	16	1.6612	0.265	0.095
						RELATIVE UPTAKE =		0.220
10	IRIDIUM	200	UNSINTERED			1.6964	1.380	0.482
	IRIDIUM	201	HYD	650	1	1.6964	1.081	0.378
	IRIDIUM	202	HYD	650	1	1.6964	1.079	0.377
						RELATIVE UPTAKE =		0.783
11	IRIDIUM	257	UNSINTERED			1.7258	1.278	0.439
	IRIDIUM	258	HYD	650	1	1.7258	1.131	0.388
	IRIDIUM	259	HYD	650	1	1.7258	1.123	0.386
						RELATIVE UPTAKE =		0.882
12	IRIDIUM	166	UNSINTERED			1.6675	1.312	0.466
	IRIDIUM	167	UNSINTERED			1.6675	1.252	0.445
	IRIDIUM	169	HYD	800	1	1.6675	0.998	0.355
	IRIDIUM	170	HYD	800	1	1.6675	0.956	0.340
						RELATIVE UPTAKE =		0.763

EXP	CAT	RUN #	PRETREATMENT ATM	TEMP (°C)	TIME (h)	SAMPLE SIZE (gm)	NUMBER OF PULSES ADSORBED	H/M
13	IRIDIUM	171	UNSINTERED			1.6616	1.309	0.467
	IRIDIUM	172	UNSINTERED			1.6616	1.280	0.456
	IRIDIUM	173	HYD	650	16	1.6616	1.061	0.378
	IRIDIUM	174	HYD	650	16	1.6616	1.064	0.379
						RELATIVE UPTAKE =		0.821
14	IRIDIUM	223	UNSINTERED			1.8039	1.328	0.436
	IRIDIUM	224	HYD	650	16	1.8039	1.069	0.351
	IRIDIUM	225	HYD	650	16	1.8039	1.061	0.349
						RELATIVE UPTAKE =		0.802
15	IRIDIUM	188	UNSINTERED			1.7258	1.402	0.481
	IRIDIUM	189	UNSINTERED			1.7258	1.358	0.466
	IRIDIUM	190	HYD	800	16	1.7258	0.840	0.288
	IRIDIUM	191	HYD	800	16	1.7258	0.835	0.287
						RELATIVE UPTAKE =		0.607
16	IRIDIUM	181	UNSINTERED			1.7059	1.304	0.453
	IRIDIUM	182	UNSINTERED			1.7059	1.275	0.443
	IRIDIUM	183	HYD	800	16	1.7059	0.806	0.280
	IRIDIUM	184	HYD	800	16	1.7059	0.806	0.280
						RELATIVE UPTAKE =		0.626

EXP	CAT	RUN #	PRETREATMENT ATM	TEMP (°C)	TIME (h)	SAMPLE SIZE (gm)	NUMBER OF PULSES ADSORBED	H/M
17	PLATINUM	263	UNSINTERED			1.6863	1.202	0.429
	PLATINUM	265	OXY	300	1	1.6863	1.185	0.423
	PLATINUM	264	OXY	300	1	1.6863	1.103	0.393
						RELATIVE UPTAKE =		0.952
18	PLATINUM	275	UNSINTERED			1.7406	1.156	0.399
	PLATINUM	276	OXY	300	1	1.7406	1.164	0.402
	PLATINUM	277	OXY	300	1	1.7406	1.210	0.418
						RELATIVE UPTAKE =		1.027
19	PLATINUM	124	UNSINTERED			1.6694	1.271	0.458
	PLATINUM	125	UNSINTERED			1.6694	1.261	0.454
	PLATINUM	126	OXY	400	1	1.6694	1.630	0.587
	PLATINUM	127	OXY	400	1	1.6694	1.571	0.566
						RELATIVE UPTAKE =		1.265
20	PLATINUM	42	UNSINTERED			1.7984	1.165	0.390
	PLATINUM	43	UNSINTERED			1.7984	1.130	0.378
	PLATINUM	44	OXY	500	1	1.7984	1.803	0.603
	PLATINUM	45	OXY	500	1	1.7984	1.685	0.563
						RELATIVE UPTAKE =		1.520

EXP	CAT	RUN #	PRETREATMENT ATM	PRETREATMENT TEMP (°C)	PRETREATMENT TIME (h)	SAMPLE SIZE (gm)	NUMBER OF PULSES ADSORBED	H/M
21	PLATINUM	50	UNSINTERED			1.7474	1.285	0.442
	PLATINUM	51	UNSINTERED			1.7474	1.308	0.450
	PLATINUM	52	OXY	600	1	1.7474	1.289	0.444
	PLATINUM	53	OXY	600	1	1.7474	1.236	0.425
							RELATIVE UPTAKE =	0.974
22	PLATINUM	57	UNSINTERED			1.7700	1.101	0.374
	PLATINUM	58	UNSINTERED			1.7700	1.024	0.348
	PLATINUM	59	OXY	700	1	1.7700	0.451	0.154
	PLATINUM	60	OXY	700	1	1.7700	0.511	0.174
							RELATIVE UPTAKE =	0.453
23	PLATINUM	266	UNSINTERED			1.7775	1.222	0.413
	PLATINUM	267	OXY	300	16	1.7775	1.295	0.438
	PLATINUM	268	OXY	300	16	1.7775	1.258	0.426
							RELATIVE UPTAKE =	1.045
24	PLATINUM	64	UNSINTERED			1.7445	1.145	0.395
	PLATINUM	65	UNSINTERED			1.7445	1.193	0.411
	PLATINUM	66	OXY	400	16	1.7445	1.468	0.506
	PLATINUM	67	OXY	400	16	1.7445	1.392	0.480
							RELATIVE UPTAKE =	1.224

EXP	CAT	RUN #	PRETREATMENT ATM	TEMP (°C)	TIME (h)	SAMPLE SIZE (gm)	NUMBER OF PULSES ADSORBED	H/M
25	PLATINUM	46	UNSINTERED			1.6678	1.089	0.393
	PLATINUM	47	UNSINTERED			1.6678	1.039	0.375
	PLATINUM	48	OXY	500	16	1.6678	2.242	0.808
	PLATINUM	49	OXY	500	16	1.6678	2.242	0.808
							RELATIVE UPTAKE =	2.108
26	PLATINUM	54	UNSINTERED			1.7056	1.063	0.375
	PLATINUM	55	OXY	600	16	1.7056	1.092	0.385
	PLATINUM	56	OXY	600	16	1.7056	1.099	0.387
							RELATIVE UPTAKE =	1.031
27	PLATINUM	61	UNSINTERED			1.6708	1.028	0.370
	PLATINUM	62	OXY	700	16	1.6708	0.325	0.117
	PLATINUM	63	OXY	700	16	1.6708	0.300	0.108
							RELATIVE UPTAKE =	0.304
28	PLATINUM	335	UNSINTERED			1.7181	1.041	0.364
	PLATINUM	336	UNSINTERED			1.7181	1.045	0.366
	PLATINUM	337	OXY	800	16	1.7181	0.170	0.060
	PLATINUM	338	OXY	800	16	1.7181	0.140	0.049
							RELATIVE UPTAKE =	0.149

EXP	CAT	RUN #	PRETREATMENT ATM	TEMP (°C)	TIME (h)	SAMPLE SIZE (gm)	NUMBER OF PULSES ADSORBED	H/M
29	PLATINUM	155	UNSINTERED			1.6938	1.300	0.461
	PLATINUM	156	UNSINTERED			1.6938	1.285	0.456
	PLATINUM	158	HYD	650	1	1.6938	1.103	0.392
	PLATINUM	159	HYD	650	1	1.6938	1.043	0.370
						RELATIVE UPTAKE =		0.831
30	PLATINUM	150	UNSINTERED			1.7917	1.350	0.453
	PLATINUM	151	UNSINTERED			1.7917	1.350	0.453
	PLATINUM	153	HYD	800	1	1.7917	0.791	0.266
	PLATINUM	154	HYD	800	1	1.7917	0.810	0.272
						RELATIVE UPTAKE =		0.593
31	PLATINUM	214	UNSINTERED			1.7593	1.079	0.369
	PLATINUM	215	HYD	650	16	1.7593	0.666	0.228
	PLATINUM	216	HYD	650	16	1.7593	0.672	0.230
						RELATIVE UPTAKE =		0.621
32	PLATINUM	160	UNSINTERED			1.5765	1.142	0.436
	PLATINUM	161	UNSINTERED			1.5765	1.116	0.426
	PLATINUM	162	HYD	650	16	1.5765	0.634	0.242
	PLATINUM	163	HYD	650	16	1.5765	0.713	0.272
						RELATIVE UPTAKE =		0.597

EXP	CAT	RUN #	PRETREATMENT ATM	TEMP (°C)	TIME (h)	SAMPLE SIZE (gm)	NUMBER OF PULSES ADSORBED	H/M
33	PLATINUM	376	UNSINTERED			1.6728	1.093	0.393
	PLATINUM	377	UNSINTERED			1.6728	1.076	0.387
	PLATINUM	378	HYD	650	16	1.6728	0.607	0.218
	PLATINUM	379	HYD	650	16	1.6728	0.649	0.234
						RELATIVE UPTAKE =		0.580
34	PLATINUM	196	UNSINTERED			1.7355	1.178	0.408
	PLATINUM	197	UNSINTERED			1.7355	1.244	0.431
	PLATINUM	198	HYD	800	16	1.7355	0.349	0.121
	PLATINUM	199	HYD	800	16	1.7355	0.338	0.117
						RELATIVE UPTAKE =		0.284

EXP	CAT	RUN #	PRETREATMENT ATM	TEMP (°C)	TIME (h)	SAMPLE SIZE (gm)	NUMBER OF PULSES ADSORBED	H/M
35	PT-IR AY	80	UNSINTERED			1.5300	2.205	0.430
	PT-IR AY	81	OXY	300	1	1.5300	2.231	0.435
	PT-IR AY	82	OXY	300	1	1.5300	2.214	0.431
						RELATIVE UPTAKE =		1.008
36	PT-IR AY	77	UNSINTERED			1.4686	2.167	0.440
	PT-IR AY	78	OXY	400	1	1.4686	1.649	0.335
	PT-IR AY	79	OXY	400	1	1.4686	1.614	0.328
						RELATIVE UPTAKE =		0.753
37	PT-IR AY	68	UNSINTERED			1.3890	2.026	0.435
	PT-IR AY	69	UNSINTERED			1.3890	2.018	0.433
	PT-IR AY	70	OXY	500	1	1.3890	1.246	0.267
	PT-IR AY	71	OXY	500	1	1.3890	1.117	0.240
						RELATIVE UPTAKE =		0.585
38	PT-IR AY	131	UNSINTERED			1.5412	2.435	0.471
	PT-IR AY	132	OXY	500	1	1.5412	1.424	0.275
	PT-IR AY	133	OXY	500	1	1.5412	1.362	0.263
						RELATIVE UPTAKE =		0.573

EXP	CAT	RUN #	PRETREATMENT ATM	TEMP (°C)	TIME (h)	SAMPLE SIZE (gm)	NUMBER OF PULSES ADSORBED	H/M
39	PT-IR AY	95	UNSINTERED			1.5593	2.299	0.439
	PT-IR AY	96	UNSINTERED			1.5593	2.266	0.433
	PT-IR AY	97	OXY	600	1	1.5593	1.350	0.258
	PT-IR AY	98	OXY	600	1	1.5593	1.373	0.262
						RELATIVE UPTAKE =		0.597
40	PT-IR AY	83	UNSINTERED			1.5261	2.184	0.427
	PT-IR AY	85	OXY	300	16	1.5261	2.256	0.441
	PT-IR AY	84	OXY	300	16	1.5261	2.310	0.451
						RELATIVE UPTAKE =		1.046
41	PT-IR AY	92	UNSINTERED			1.3551	1.868	0.411
	PT-IR AY	93	OXY	400	16	1.3551	1.129	0.248
	PT-IR AY	94	OXY	400	16	1.3551	1.142	0.251
						RELATIVE UPTAKE =		0.608
42	PT-IR AY	75	UNSINTERED			1.2851	2.035	0.472
	PT-IR AY	76	OXY	400	16	1.3851	1.298	0.279
	PT-IR AY	76A	OXY	400	16	1.3851	1.180	0.254
						RELATIVE UPTAKE =		0.565

EXP	CAT	RUN #	PRETREATMENT ATM	PRETREATMENT TEMP (°C)	PRETREATMENT TIME (h)	SAMPLE SIZE (gm)	NUMBER OF PULSES ADSORBED	H/M
43	PT-IR AY	85A	UNSINTERED			1.4358	2.188	0.454
	PT-IR AY	86	UNSINTERED			1.4358	1.805	0.375
	PT-IR AY	87	OXY	500	16	1.4358	1.728	0.359
	PT-IR AY	88	OXY	500	16	1.4358	1.820	0.378
						RELATIVE UPTAKE =		0.889
44	PT-IR AY	128	UNSINTERED			1.5087	2.169	0.428
	PT-IR AY	129	OXY	500	16	1.5087	2.010	0.397
	PT-IR AY	130	OXY	500	16	1.5087	1.952	0.386
						RELATIVE UPTAKE =		0.914
45	PT-IR AY	369	UNSINTERED			1.6224	2.224	0.409
	PT-IR AY	370	UNSINTERED			1.6224	2.175	0.400
	PT-IR AY	371	OXY	500	16	1.6224	2.009	0.369
	PT-IR AY	372	OXY	500	16	1.6224	1.924	0.353
						RELATIVE UPTAKE =		0.895
46	PT-IR AY	89	UNSINTERED			1.4618	2.152	0.439
	PT-IR AY	90	OXY	600	16	1.4618	1.123	0.229
	PT-IR AY	90	OXY	600	16	1.4618	1.123	0.229
						RELATIVE UPTAKE =		0.522

EXP	CAT	RUN #	PRETREATMENT ATM	TEMP (°C)	TIME (h)	SAMPLE SIZE (gm)	NUMBER OF PULSES ADSORBED	H/M
47	PT-IR AY	203	UNSINTERED			1.4024	1.968	0.418
	PT-IR AY	204	HYD	650	1	1.4024	1.657	0.352
	PT-IR AY	205	HYD	650	1	1.4024	1.685	0.358
						RELATIVE UPTAKE =		0.850
48	PT-IR AY	185	UNSINTERED			1.3326	1.879	0.420
	PT-IR AY	186	HYD	800	1	1.3326	1.403	0.314
	PT-IR AY	187	HYD	800	1	1.3326	1.384	0.310
						RELATIVE UPTAKE =		0.742
49	PT-IR AY	210	UNSINTERED			1.4500	2.009	0.413
	PT-IR AY	211	UNSINTERED			1.4500	1.970	0.405
	PT-IR AY	212	HYD	650	16	1.4500	1.652	0.340
	PT-IR AY	213	HYD	650	16	1.4500	1.572	0.323
						RELATIVE UPTAKE =		0.811
50	PT-IR AY	216	UNSINTERED			1.3885	1.901	0.408
	PT-IR AY	217	HYD	800	16	1.3885	1.207	0.259
	PT-IR AY	218	HYD	800	16	1.3885	1.183	0.254
						RELATIVE UPTAKE =		0.629

EXP	CAT	RUN #	PRETREATMENT ATM	TEMP (°C)	TIME (h)	SAMPLE SIZE (gm)	NUMBER OF PULSES ADSORBED	H/M
51	PT-IR MX	146	UNSINTERED			1.6839	1.295	0.458
	PT-IR MX	147	UNSINTERED			1.6839	1.235	0.437
	PT-IR MX	148	OXY	300	1	1.6839	1.293	0.458
	PT-IR MX	149	OXY	300	1	1.6839	1.350	0.478
							RELATIVE UPTAKE =	1.045
52	PT-IR MX	269	UNSINTERED			1.7485	1.275	0.435
	PT-IR MX	270	OXY	400	1	1.7485	1.099	0.375
	PT-IR MX	270	OXY	400	1	1.7485	1.099	0.375
							RELATIVE UPTAKE =	0.862
53	PT-IR MX	138	UNSINTERED			1.6622	1.273	0.457
	PT-IR MX	139	UNSINTERED			1.6622	1.201	0.431
	PT-IR MX	140	OXY	400	1	1.6622	1.100	0.394
	PT-IR MX	141	OXY	400	1	1.6622	0.994	0.356
							RELATIVE UPTAKE =	0.847
54	PT-IR MX	134	UNSINTERED			1.6759	1.166	0.415
	PT-IR MX	135	UNSINTERED			1.6759	1.166	0.415
	PT-IR MX	136	OXY	500	1	1.6759	1.171	0.417
	PT-IR MX	137	OXY	500	1	1.6759	1.161	0.413
							RELATIVE UPTAKE =	1.000

EXP	CAT	RUN #	PRETREATMENT ATM	TEMP (°C)	TIME (h)	SAMPLE SIZE (gm)	NUMBER OF PULSES ADSORBED	H/M
55	PT-IR MX	142	UNSINTERED			1.7402	1.251	0.429
	PT-IR MX	143	UNSINTERED			1.7402	1.230	0.421
	PT-IR MX	144	OXY	600	1	1.7402	0.935	0.320
	PT-IR MX	145	OXY	600	1	1.7402	0.914	0.313
						RELATIVE UPTAKE =		0.746
56	PT-IR MX	107	UNSINTERED			1.7598	1.437	0.487
	PT-IR MX	108	UNSINTERED			1.7598	1.395	0.473
	PT-IR MX	110	OXY	300	16	1.7598	1.546	0.524
	PT-IR MX	111	OXY	300	16	1.7598	1.493	0.506
						RELATIVE UPTAKE =		1.074
57	PT-IR MX	103	UNSINTERED			1.8351	1.459	0.474
	PT-IR MX	104	UNSINTERED			1.8351	1.417	0.460
	PT-IR MX	105	OXY	400	16	1.8351	1.194	0.388
	PT-IR MX	106	OXY	400	16	1.8351	1.120	0.364
						RELATIVE UPTAKE =		0.805
58	PT-IR MX	99	UNSINTERED			1.9781	1.514	0.456
	PT-IR MX	100	UNSINTERED			1.9781	1.481	0.446
	PT-IR MX	101	OXY	500	16	1.9781	1.577	0.475
	PT-IR MX	102	OXY	500	16	1.9781	1.653	0.498
						RELATIVE UPTAKE =		1.079

EXP	CAT	RUN #	PRETREATMENT ATM	TEMP (C)	TIME (h)	SAMPLE SIZE (gm)	NUMBER OF PULSES ADSORBED	H/M
59	PT-IR MX	112	UNSINTERED			1.7094	1.136	0.396
	PT-IR MX	113	UNSINTERED			1.7094	1.118	0.390
	PT-IR MX	114	OXY	600	16	1.7094	0.822	0.287
	PT-IR MX	115	OXY	600	16	1.7094	0.832	0.290
						RELATIVE UPTAKE =		0.734
60	PT-IR MX	204	UNSINTERED			1.8252	1.304	0.426
	PT-IR MX	205	HYD	650	1	1.8252	1.066	0.348
	PT-IR MX	206	HYD	650	1	1.8252	1.063	0.347
						RELATIVE UPTAKE =		0.817
61	PT-IR MX	373	UNSINTERED			1.8320	1.353	0.440
	PT-IR MX	374	HYD	800	1	1.8320	0.910	0.296
	PT-IR MX	375	HYD	800	1	1.8320	0.926	0.301
						RELATIVE UPTAKE =		0.679
62	PT-IR MX	192	UNSINTERED			1.7975	1.309	0.434
	PT-IR MX	193	UNSINTERED			1.7975	1.256	0.417
	PT-IR MX	194	HYD	650	16	1.7975	0.905	0.300
	PT-IR MX	195	HYD	650	16	1.7975	0.907	0.301
						RELATIVE UPTAKE =		0.707

EXP	CAT	RUN #	PRETREATMENT ATM	PRETREATMENT TEMP (°C)	PRETREATMENT TIME (h)	SAMPLE SIZE (gm)	NUMBER OF PULSES ADSORBED	H/M
63	PT-IR MX	219	UNSINTERED			1.6120	1.175	0.434
	PT-IR MX	220	UNSINTERED			1.6120	1.160	0.429
	PT-IR MX	221	HYD	800	16	1.6120	0.563	0.208
	PT-IR MX	222	HYD	800	16	1.6120	0.632	0.234

RELATIVE UPTAKE = 0.512

EXP	CAT	RUN #	PRETREATMENT ATM	TEMP (°C)	TIME (h)	SAMPLE SIZE (gm)	NUMBER OF PULSES ADSORBED	H/M
64	PT-W AY	317	UNSINTERED			2.4814	0.490	0.058
	PT-W AY	318	OXY	400	1	2.4814	0.487	0.057
	PT-W AY	319	OXY	400	1	2.4814	0.582	0.068
						RELATIVE UPTAKE =		1.091
65	PT-W AY	320	UNSINTERED			2.4908	0.456	0.053
	PT-W AY	321	OXY	500	1	2.4908	0.954	0.112
	PT-W AY	322	OXY	500	1	2.4908	0.891	0.104
						RELATIVE UPTAKE =		2.024
66	PT-W AY	343	UNSINTERED			2.4940	0.436	0.051
	PT-W AY	344	OXY	600	1	2.4940	1.106	0.129
	PT-W AY	345	OXY	600	1	2.4940	1.112	0.130
						RELATIVE UPTAKE =		2.544
67	PT-W AY	354	UNSINTERED			2.5375	0.421	0.048
	PT-W AY	355	OXY	600	1	2.5375	1.104	0.127
	PT-W AY	355	OXY	600	1	2.5375	1.104	0.127
						RELATIVE UPTAKE =		2.623

EXP	CAT	RUN #	PRETREATMENT ATM	TEMP (°C)	TIME (h)	SAMPLE SIZE (gm)	NUMBER OF PULSES ADSORBED	H/M
68	PT-W AY	356	UNSINTERED			2.5112	0.456	0.053
	PT-W AY	357	OXY	700	1	2.5112	0.458	0.053
	PT-W AY	358	OXY	700	1	2.5112	0.497	0.058
						RELATIVE UPTAKE =		1.048
69	PT-W AY	361	UNSINTERED			2.5684	0.704	0.080
	PT-W AY	362	UNSINTERED			2.5684	0.815	0.092
	PT-W AY	363	OXY	600	16	2.5684	1.256	0.142
	PT-W AY	364	OXY	600	16	2.5684	1.340	0.152
						RELATIVE UPTAKE =		1.710
70	PT-W AY	365	UNSINTERED			2.4844	0.592	0.069
	PT-W AY	366	UNSINTERED			2.4844	0.557	0.065
	PT-W AY	367	OXY	600	16	2.4844	1.128	0.132
	PT-W AY	368	OXY	600	16	2.4844	1.149	0.135
						RELATIVE UPTAKE =		1.982
71	PT-W AY	313	UNSINTERED			2.4982	0.391	0.046
	PT-W AY	314	UNSINTERED			2.4982	0.390	0.045
	PT-W AY	315	HYD	650	1	2.4982	0.317	0.037
	PT-W AY	316	HYD	650	1	2.4982	0.352	0.041
						RELATIVE UPTAKE =		0.857

EXP	CAT	RUN #	PRETREATMENT ATM	TEMP (°C)	TIME (h)	SAMPLE SIZE (gm)	NUMBER OF PULSES ADSORBED	H/M
72	PT-W AY	327	UNSINTERED			2.4975	0.473	0.055
	PT-W AY	328	HYD	800	1	2.4975	0.122	0.014
	PT-W AY	329	HYD	800	1	2.4975	0.141	0.016

RELATIVE UPTAKE = 0.279

EXP	CAT	RUN #	PRETREATMENT ATM	TEMP (°C)	TIME (h)	SAMPLE SIZE (gm)	NUMBER OF PULSES ADSORBED	H/M
73	PT-W MX	351	UNSINTERED			3.4451	1.132	0.191
	PT-W MX	352	OXY	400	1	3.4451	1.108	0.187
	PT-W MX	353	OXY	400	1	3.4451	1.140	0.193
						RELATIVE UPTAKE =		0.993
74	PT-W MX	239	UNSINTERED			2.7090	1.020	0.219
	PT-W MX	240	OXY	500	1	2.7090	1.614	0.347
	PT-W MX	241	OXY	500	1	2.7090	1.581	0.340
						RELATIVE UPTAKE =		1.567
75	PT-W MX	349	UNSINTERED			3.4124	1.359	0.232
	PT-W MX	350	OXY	600	1	3.4124	1.527	0.261
	PT-W MX	350	OXY	600	1	3.4124	1.527	0.261
						RELATIVE UPTAKE =		1.124
76	PT-W MX	359	UNSINTERED			3.4187	1.292	0.220
	PT-W MX	360	OXY	700	1	3.4187	0.563	0.096
	PT-W MX	360	OXY	700	1	3.4187	0.563	0.096
						RELATIVE UPTAKE =		0.436

EXP	CAT	RUN #	PRETREATMENT ATM	TEMP (°C)	TIME (h)	SAMPLE SIZE (gm)	NUMBER OF PULSES ADSORBED	H/M
77	PT-W MX	309	UNSINTERED			3.3858	1.146	0.197
	PT-W MX	310	UNSINTERED			3.3858	1.139	0.196
	PT-W MX	311	OXY	400	16	3.3858	1.203	0.207
	PT-W MX	312	OXY	400	16	3.3858	1.284	0.221
						RELATIVE UPTAKE =		1.089
78	PT-W MX	245	UNSINTERED			2.9834	1.018	0.199
	PT-W MX	246	UNSINTERED			2.9834	1.018	0.199
	PT-W MX	247	OXY	650	16	2.9834	0.643	0.126
	PT-W MX	248	OXY	650	16	2.9834	0.671	0.131
						RELATIVE UPTAKE =		0.646
79	PT-W MX	346	UNSINTERED			3.4206	1.377	0.235
	PT-W MX	347	HYD	650	1	3.4206	0.811	0.138
	PT-W MX	348	HYD	650	1	3.4206	0.884	0.151
						RELATIVE UPTAKE =		0.616
80	PT-W MX	330	UNSINTERED			3.2604	1.097	0.196
	PT-W MX	331	HYD	800	1	3.2604	0.515	0.092
	PT-W MX	332	HYD	800	1	3.2604	0.593	0.106
						RELATIVE UPTAKE =		0.506

EXP	CAT	RUN #	PRETREATMENT ATM	TEMP (°C)	TIME (h)	SAMPLE SIZE (gm)	NUMBER OF PULSES ADSORBED	H/M
81	PT-W MX	323	UNSINTERED			3.2535	1.026	0.184
	PT-W MX	324	UNSINTERED			3.2535	1.046	0.187
	PT-W MX	325	HYD	650	16	3.2535	0.511	0.092
	PT-W MX	326	HYD	650	16	3.2535	0.549	0.098
							RELATIVE UPTAKE =	0.512
82	PT-W MX	243	UNSINTERED			2.4340	0.873	0.209
	PT-W MX	244	HYD	800	16	2.3430	0.235	0.058
	PT-W MX	244	HYD	800	16	2.3430	0.235	0.058
							RELATIVE UPTAKE =	0.280

Table B-2

The Experiments Omitted from the Chemisorption Data in Table B-1

Run #	Cat	Treatment Atm	Temp (°C)	Time (h)	Reason for Omission
178-180	Ir	HYD	650	1	The initial uptake (H/M) was too low. (i.e. 0.233)
150-152	Pt	HYD	800	1	The 2nd H_2 adsorption on the sintered sample was 30% more than the 1st adsorption.
164-165	Pt	HYD	650	16	The relative uptake was much higher than the other 3 experiments at this sintering condition.
72-74	Pt-Ir AY	OXY	500	16	The initial uptake (H/M) was too low. (i.e. 0.271)
207-209	Pt-Ir MX	HYD	800	1	The relative uptake of 0.531 did not seem to 'fit' as indicated by the other results.
116-119	Ir	OXY	500	4	This Ir sample was sintered for 4 hrs.
340-342	Pt-W MX	OXY	400	1	The initial uptake (H/M) was too high. (i.e. 0.286)

Table B-3
Computer Programs

The following are the programs were used to calculate the H/M ratios for the different catalysts. Program 1 was used to calculate the H/M for the monometallic catalysts. Program 2 was used to calculate the H/M for the bimetallic and the mechanically mixed catalysts.

The first piece of data to be read by the programs is the atomic weight of the metal used in the catalyst. In program 1 this is designated as XWT and has a format of F10.3. For program 2 the atomic weight of the metal is designated as XWT1, has a F10.3 format and is either the atomic weight of Ir or W. The atomic weight of Pt has already been incorporated into program 2. The next input string of data required by both programs 1 and 2 are given in Table B-3.1.

Table B-3.1
Input Format

Input	Columns	Format	Name in Program
catalyst identification	1-8	2A4	CATID1,CATID2
experiment run #	9-12	A4	RN
sintering atmosphere	13-16	A4	ATM
sintering temperature in C	17-20	A4	TEMP
sintering time either 1 or 16 hrs.	21-24	A4	TIME
catalyst weight	25-34	F10.4	CATWT
ambient pressure	35-44	F10.4	PRESS
ambient temperature	45-54	F10.4	ATEMP
no. of pulses adsorbed	55-64	F10.4	PULSE
% metal on catalyst	65-66	I2	ID
no. of H_2 titrations on the unsintered sample	67-68	I2	IX

Note that all the A format were right justified when entered. The program can take one or two sets of data for the unsintered sample. However it was assumed that there would always be two measurements on the sintered sample. In the few cases where a repeat measurement was not made, the data were just entered twice.

The ambient temperature and pressure were entered into the data just for reference. They were not used in the calculations.

In the following programs the 'I' is a counter which can be set to any interger value and from which the experiments in the data set are numbered consecutively.

PROGRAM 1

```
      I=1
116   N=0
      WRITE(6,6001)
      WRITE(6,6002)
      WRITE(6,6003)
110   M=0
      US=0.0
      S=0.0
      READ(5,5001)  XWT
108   READ(5,5002,END=999)CATID1,CATID2,RN,ATM,TEMP,TIME,CATWT,PRESS,
     CATEMP,PULSE,ID,IX
      M=M+1
      IF(ID-1) 103,103,104
103   X=0.01
      GO TO 401
104   X=0.02
401       U=(PULSE*0.345/22414.0)*2.0/(CATWT*X/XWT)+0.0005
      IF(M.EQ.1)  GO TO 100
      IF(2-M) 101,102,102
102   US=(PULSE*0.345/22414.0)*2.0/(CATWT*X*1.0/XWT)+US
      GO TO 107
101   S=(PULSE*0.345/22414.0)*2.0/(CATWT*X*1.0/XWT)+S
106   GO TO 109
105   RU=S/US+0.0005
      I=I+1
      WRITE(6,6005)RU
      WRITE(6,6006)
      N=N+1
      IF(3-N)  114,115,115
114   GO TO 116
115   GO TO 110
107   WRITE(6,6004)CATID1,CATID2,RN,ATM,TEMP,TIME,CATWT,PULSE,U
120      IF(IX-1) 111,111,112
111   US=2.0*US
      M=M+1
```

cont'd

```
112  GO TO 108
109  WRITE(6,6004)CATID1,CATID2,RN,ATM,TEMP,TIME,CATWT,PULSE,U
     IF(4-M) 105,105,108
100  WRITE(6,6010)I,CATID1,CATID2,RN,ATM,TEMP,TIME,CATWT,PULSE,U
     US=(PULSE*0.345/22414.0)*2.0/(CATWT*X*1.0/XWT)+US
      GO TO 120
 113 STOP
6010  FORMAT(/,10X,I2,4X,2A4,2X,A4,2X,3A4,3X,1F7.4,3X,1F6.3,2X,1F6.3,/)
6004 FORMAT(16X,2A4,2X,A4,2X,3A4,3X,1F7.4,3X,1F6.3,2X,1F6.3,/)
6006 FORMAT(/)
6005 FORMAT(/,48X,'RELATIVE UPTAKE =',1F6.3)
5001 FORMAT(F10.3)
5002 FORMAT(2A4,4A4,4F10.4,I2,I2)
6003 FORMAT(28X,'#          (C)   (HR)    (GM)    ADSORBED',//)
6002 FORMAT(10X,'EXP     CAT        RUN    ATM TEMP TIME    SIZE    OF PULSE
    CS')
6001 FORMAT('1',///,34X,'PRETREATMENT  SAMPLE    NUMBER      H/E')
999  STOP
     END
```

PROGRAM 2

```
      I=1
116   N=0
      WRITE(6,6001)
      WRITE(6,6002)
      WRITE(6,6003)
110   M=0
      US=0.0
      S=0.0
     READ(5,5001) XWT1
      XWT2=195.09
108   READ(5,5002,END=999)CATID1,CATID2,RN,ATM,TEMP,TIME,CATWT,PRESS,
     CATEMP,PULSE,ID,IX
      M=M+1
      IF(ID-1)103,103,104
103   X=0.01
      GO TO 401
104   X=0.02
401   U=(PULSE*0.345/22414.0)*2.0/((CATWT*X/2.0)*(1.0/XWT1+1.0/XWT2))+0.0005
      IF(M.EQ.1) GO TO 100
      IF(2-M)101,102,102
102   US=(PULSE*0.345/22414.)*2./((CATWT*X/2.0)*(1.0/XWT1+1.0/XWT2))+US
      GO TO 107
101   S=(PULSE*0.345/22414.0)*2.0/((CATWT*X/2.0)*(1.0/XWT1+1.0/XWT2))+S
106   GO TO 109
105   RU=S/US+0.0005
      I=I+1
      WRITE(6,6005)RU
      WRITE(6,6006)
      N=N+1
      IF(3-N) 114,115,115
114   GO TO 116
115   GO TO 110
107   WRITE(6,6004)CATID1,CATID2,RN,ATM,TEMP,TIME,CATWT,PULSE,U
120   IF(IX-1)111,111,112
```

cont'd

```
111  US=2.0*US
     M=M+1
112  GO TO 108
109  WRITE(6,6004)CATID1,CATID2,RN,ATM,TEMP,TIME,CATWT,PULSE,U
     IF(4-M) 105,105,108
100  WRITE(6,6010)I,CATID1,CATID2,RN,ATM,TEMP,TIME,CATWT,PULSE,U
     US=(PULSE*0.345/22414.)*2./((CATWT*X/2.0)*(1.0/XWT1+1.0/XWT2))+US
      GO TO 120
113  STOP
6010 FORMAT(/,10X,I2,4X,2A4,2X,A4,2X,3A4,3X,1F7.4,3X,1F6.3,2X,1F6.3,/)
6004 FORMAT(16X,2A4,2X,A4,2X,3A4,3X,1F7.4,3X,1F6.3,2X,1F6.3,/)
6006 FORMAT(/)
6005 FORMAT(/,48X,'RELATIVE UPTAKE =',1F6.3)
5001 FORMAT(F10.3)
5002 FORMAT(2A4,4A4,4F10.4,I2,I2)
6003 FORMAT(28X,'#          (C)   (HR)    (GM)    ADSORBED',//)
6002 FORMAT(10X,'EXP    CAT        RUN    ATM TEMP TIME    SIZE    OF PULSE
    CS')
6001 FORMAT('1',///,34X,'PRETREATMENT  SAMPLE   NUMBER      H/M')
999  STOP
     END
```

APPENDIX C

C-1 Tungsten Analysis

In a procedure similar to that used by Mertzweiller(18), ammonium metatungstate was used to impregnate the Alon with tungsten. The molecular formula for ammonium metatungstate is: $(NH_4)_6W_{12}O_{39}$. Because of its affinity for water and its easy hydrolysis to tungstic acid and other polytungstates(55) the purity of the sample as $(NH_4)_6W_{12}O_{39}$ could not be guaranteed. In order to find the tungsten content the metatungstate was pyrolized to give WO_3 . The reaction is:

$$(NH_4)_6W_{12}O_{39} \longrightarrow 6NH_3 + 12\,WO_3 + 3H_2O \qquad (C-1)$$

Other polytungstates and tungstic acid decompose with heat in a similar fashion to give WO_3 (55).

Approximately 0.3 grams of ammonium metatungstate was accurately weighed into a previously fired and weighed crucible. The crucible plus contents was placed in a muffle furnace at 600 °C and left overnight. The crucilble was removed and allowed to cool in a dessicator. The crucible and contents were weighed again and then placed back in the muffle furnace for several more hours so as to check that reaction C-1 was complete. The analysis was done in duplicate. The calculation of the wt.% tungsten in the ammonium metatungstate

was based on the assumption that the contents in the crucible after heating in the furnace was WO_3. The wt.% tungsten was found to be 72.6 +/- 0.01 compared to the theoretical wt.% W based on the formula $(NH_4)_6W_{12}O_{39}$ which is 75.1.

C-2 Reduction of WCl_6 to W In situ

It was found in the literature (24,25) that the impregnation of alumina with an aqueous solution of ammonium metatungstate followed by drying and reduction in hydrogen, resulted in a reaction of the tungsten with the alumina. It was not clear whether this reaction was a result of the compound used to impregnate the alumina, or due to other factors such as the presence of water or oxygen or whether it was just the chemical nature of the W/ Al_2O_3 system. Because of the successful preparation of the Pt and Ir catalysts with $PtCl_2$ and $IrCl_3$, it was decided to impregnate the Alon with WCl_6. Further, the reduction was attempted in situ.

The procedure was as follows: A weighed amount of dry Alon was placed in a three necked 250 ml round bottomed flask. Two of the necks of the flask were fitted so as to act as an inlet and outlet port for dry nitrogen purge gas. The third neck of the flask was fitted with a 125 ml cylindrical separatory funnel. WCl_6 is not soluble in water and thus was used as the solvent. The CCl_4 was spectral quality (Fisher Scientific Co., Fairlawn, New Jersey) and was dried with molecular sieves. An amount of WCl_6 was dissolved into

100 ml of CCl_4 so as to give a 1wt% W loading to the Alon. The CCl_4 / WCl_6 solution was kept as free from exposure to water as possible. The solution was added slowly to the Alon which was being purged by dry nitrogen and also stirred with a magnetic stirrer. The solution was allowed to impregnate the Alon for 1 hr. At this point the nitrogen flow was stopped and a gentle vacuum was attached to the outlet port of the flask. A heating mantel was used to heat the flask and help distill off the CCl_4. When most of the CCl_4 had been removed the vacuum was shut off and the flask was purged with H_2. The heat to the flask was increased so as to promote the reduction of the tungsten.

This method was attempted three times. Each time when the dark coloured CCl_4/ WCl_6 solution was added to the Alon and heat applied from the heating mantel, the solution went clear. No reduction to metallic tungsten was ever achieved in the three attempts. It was concluded that WCl_6 also reacts with the Alon to give a irreducible form of tungsten.